Decision Support System for Adaptive Restoration Control of Distribution System

Lili Hao, Yusheng Xue, Ze Li, Haohao Wang, and Qun Xu

***Abstract*—Aiming at the high-dimensional uncertainties of restoration process, an optimization model for distribution system restoration control is proposed considering expected restoration benefits, expected restoration costs, and security risks of the overall restoration scheme. In the proposed model, the effect of security control on restoration process is actively analyzed considering the security control costs of preventive, emergency, and correction controls. A two-layer decision support framework for distribution system restoration decision support system (DRDSS) is also designed. The upper layer of the proposed framework generates the pre-adjustment schemes of operation mode for energized power grid by load transfer and selects the optimal pre-adjustment scheme and the corresponding partitioning scheme based on the partition adjustment results of each pre-adjustment scheme. In addition, it optimizes the spatial-temporal decision-making of the inter-partition connectivity. For each partition, the lower layer of the proposed framework pre-selects the units and loads to be restored according to the pre-evaluated restoration income, generates the table of alternative restoration scheme for coping with uncertain events through simulation and deduction, and evaluates the risk and benefit of each scheme. For the uncertain events in the actual restoration process, the current restoration scheme can be adaptively switched to a sub-optimal scheme or re-optimized if necessary. Meanwhile, the proposed framework provides an information interaction interface for collaborative restoration with the related transmission system. A 123-node test system is built to evaluate the effectiveness and adaptability of the proposed model and framework.**

***Index Terms*—Distribution system, restoration, pre-adjustment of operation mode, load transfer, dynamic partitioning, risk and benefit, security control.**

I. Introduction

In case of a blackout, the restoration control of a distribution system is used to quickly restore the power supply in a safe and efficient manner to reduce the outage losses and mitigate the security risks in the restoration process [1]. Based on the local information such as adjacent bus voltage, line current, switch state, etc., the feeder-level power outage can be quickly restored by the devices of automatic reclosing, standby automatic switching, and feeder automation according to the preset logic operations [2]. For rapid restoration of a large-scale distribution power outage, it is necessary to comprehensively consider multiple independent partitions formed by the power delivery plan of the transmission system [3] at each transmission-distribution interfacing bus (TDB), black start resources [4], and microgrids [5] in the distribution system. It is noteworthy that all the partitions are restored in parallel and connected promptly to continuously expand the scope of restoration. According to the IEEE standard 1547 [6], each distributed generation (DG) in the network should be automatically disconnected after a severe disturbance. If certain conditions are met such as *v-f* control capability, etc., DGs can form intentional island to supply power to the load in advance [7]. During the restoration period, it is essential to manage high-dimensional uncertainties regarding outage scenarios, external environment, and restoration processes. The uncertainty of outage scenarios mainly refers to the spatial-temporal uncertainty of the topology, model parameters, and node power injection of the energized power grid. The external environment uncertainty is reflected in the influence of uncertain external natural disasters on the operation state and failure probability of power equipment and communication systems. The uncertainty of restoration process mainly refers to the uncertainty of the restoration operation results, including whether the local automatic device or field staff can successfully complete the restoration operation, the time of restoration operation, whether the voltage or frequency problem occurs after the restoration operation, whether various failures occur during the restoration operation, and whether the safety control measures can maintain the safe operation of the system after the failures, etc. Therefore, distribution system restoration is regarded as a multi-level, multi-region, multi-stage, strongly uncertain, nonlinear, and high-dimensional optimization problem [8]. The major optimization objectives of this problem include the minimization of load outage loss [9] and the number of switching operations required for restoration [10]. The restoration schemes are usually optimized based on mathematical programming [11], heuristic methods [12], or meta-heuristic methods [13].

Distribution networks generally adopt closed-loop design

Manuscript received: August 2, 2021; revised: January 12, 2022; accepted: March 10, 2022. Date of CrossCheck: March 10, 2022. Date of online publication: June 27, 2022.

This work was supported in part by the China State Grid Corporation project of the Key Technologies of Power Grid Proactive Support for Energy Transition (No. 5100-202040325A-0-0-00).

L. Hao is with the School of Electrical Engineering and Control Science, Nanjing Tech University, Nanjing 211816, China (e-mail: haolili@njtech.edu.cn).

Y. Xue (corresponding author), Z. Li, and H. Wang are with State Grid Electric Power Research Institute (NARI Group Corporation), Nanjing, China, and they are also with State Key Laboratory of Smart Grid Protection and Operation Control, Nanjing, China (e-mail: xueyusheng@sgepri.sgcc.com.cn; lizeseu@163.com; wanghaohao@sgepri.sgcc.com.cn).

Q. Xu is with State Grid Qingdao Power Supply Company, Qingdao, China (e-mail: xuqunxuqun@sina.com).

DOI: 10.35833/MPCE.2021.000528

and open-loop operation mode. It is notable that, in order to prevent closed-loop operation mode in the distribution network, the power grid supplied by one TDB should be restored according to its own partition and independent from power grids supplied by other TDBs. The action of matching the available power supplies and restoration targets through partitioning affects the restoration decision-making space of each partition and the global load restoration income of the distribution system. In [14], the partitions are determined according to the fixed power supply scope of each TDB during normal operation, which is unable to adapt to uncertain outage scenarios. In [15], a partitioning method is proposed based on expert knowledge considering various factors such as power supply margin, distribution network topology, and typical power supply mode. In [16], the DG partitions are divided based on heuristic method, whereas the division of overlapping areas among partitions is not mentioned. The restoration schemes of power supplies are uniformly optimized from the whole network perspective by using mathematical programming methods in [17], [18]. It is notable that the aforementioned works do not consider the time variability of neither the restoration income per unit load nor the power delivery from the transmission system to the distribution system at TDBs.

Most of the existing studies attempt to optimize the partitions and restoration schemes based on a single outage scenario. The time-varying characteristics of loads in distribution system, restoration income per unit load, power delivery from transmission system to distribution system at each TDB, along with the uncertainties in the restoration process may lead to the mismatch in available power capacity, distribution network topology, and load demand. Thus, there is a space for optimizing and adjusting system operation mode of energized power grids in a certain outage scenario. Based on a real-time outage scenario, more hypothetical scenarios are provided for dynamic partitioning by optimizing pre-adjustment schemes of operation mode for energized power grids, to supplement more matching options between available power sources and restoration targets. Currently, there are a few studies which provide a detail on this. For instance, [15] proposes a method which transfers the loads in the restored power grid, where the operating conditions reach the limits to other restored power grids to improve its power supply margin.

Considering the high-dimensional uncertainties in the restoration process, the probability and risk of load restoration delay are considered in the decision-making process in [19], whereas the impacts of uncertain events on the security risks of the distribution system are not considered. In [20], the restoration schemes are re-optimized to cope with the uncertain events in the restoration process without distinguishing the characteristics and influences of various uncertain events, which makes it hard to manage and control the restoration process adaptively.

The uncertain events in the restoration process may trigger preventive control, emergency control, or correction control to ensure operation security of power system, which is called security control in this paper. It is obvious that the security control significantly influences the restoration control process. However, its results are only reflected in the initial conditions of the restoration control [1], and the consequences and impacts of security control are not considered in the restoration decision-making and implementation processes, which seriously affects the evaluation and implementation process of the restoration schemes.

Our research group has established a transmission system restoration decision support system (TRDSS) [21]. Based on this, in order to address the aforementioned restoration control problems of distribution system, a unified risk optimization model for quantifying the economy and security of the restoration scheme is established in this paper, and a two-layer framework for the distribution system restoration decision support system (DRDSS) is further designed. The upper layer optimizes the pre-adjustment schemes of operation mode for the energized power grid, dynamically adjusts the partitions, and then performs the spatial-temporal decision-making of inter-partition connectivity. The lower layer optimizes the restoration schemes of the units and loads for each partition. At the same time, considering the possibility of collaborative restoration control of transmission and distribution systems, the information interaction interface of collaborative restoration with related transmission system is reserved, and the interaction information is discussed. The major contributions of this paper are summarized as follows.

1) Taking the maximization of the estimated restoration income as the optimization objective, an optimization method for operation mode of pre-adjustment scheme based on energized load transfer demand index is proposed. This method enables us to optimize the allocation of capacities of available power supplies from a global perspective on the basis of real-time outage scenario. Moreover, this method expands the outage scenario for dynamic partitioning from a single real-time outage scenario to a set of pre-adjusted outage scenarios.

2) The index of estimated restoration income to evaluate the partitioning effect is established, and a strategy for dividing the overlapping areas based on the guidance of branch restoration value is also proposed. Considering the time-varying characteristics of both restoration income per unit load and power delivery from transmission system to distribution system at TDB, the set of pre-adjusted outage scenarios and partitioning results are optimized to maximize the global restoration income.

3) Aiming at the high-dimensional uncertainties in the process of optimizing intra-partition restoration schemes, a table of alternative restoration scheme for dealing with uncertain events is generated through preferring the restoration targets, simulating, and deducing the restoration paths based on the unified optimization model considering security risks, and the risks and incomes of the schemes are evaluated. The risk evaluation considers the costs of preventive control, emergency control, and correction control of the restoration path.

4) Aiming at the high-dimensional uncertainties in the implementation process of restoration scheme, an adaptive management and control strategy for multi-partition collaborative restoration is established. This strategy considers the security control measures in the restoration process, quantitatively evaluates the impact of uncertain events on power grid secu-

rity and restoration process, and dynamically adjusts the partitions and the intra-partition restoration schemes.

II. Optimization Model for Distribution System Restoration

A. Relationship Between Restoration Control and Security Control

In the implementation process of restoration control, the online defense system performs the security control, including the preventive control, emergency control, and correction control, based on the power grid operation conditions and uncertain events. Therefore, the adjustment of adaptive restoration scheme according to the restoration process should consider not only the uncertain events but also the security control measures taken after uncertain events.

In the decision-making process of restoration control, for the restoration scheme that is unable to satisfy the security constraints, the optimal preventive control measures that can make the constraints satisfied can be searched and used as a part of restoration scheme. Then, the costs of the optimal preventive control measures can be added to the restoration cost. Consequently, the scheme screening based on rigid constraint check is transformed into the optimization of restoration scheme considering the preventive control costs. This expands the decision-making space of restoration schemes. The restoration scheme involves a series of restoration operations. In view of the possible security problems during the operation of the restoration scheme, the probability of the event causing the security problem, and the optimal emergency control costs or optimal correction control costs needed to keep the system safe after the event are calculated to evaluate the risk of the restoration scheme, so that the restoration scheme can be evaluated more comprehensively by introducing the security risk.

B. Mathematical Model

1) Objective Function

The optimization objective of the distribution system restoration control is to maximize the expected net income of the overall restoration scheme, which is mathematically expressed as:

$$\max_{\boldsymbol{u}^k} \sum_{k=1}^{N_\mathrm{K}} (I_\mathrm{L}^k(\boldsymbol{x}^k,\boldsymbol{u}^k,\boldsymbol{p}^k) - C^k(\boldsymbol{x}^k,\boldsymbol{u}^k,\boldsymbol{p}^k) - R^k(\boldsymbol{x}^k,\boldsymbol{u}^k,\boldsymbol{p}^k)) \quad (1)$$

where $k = 1, 2, \ldots, N_\mathrm{K}$ is the step number in the restoration scheme, and each step refers to a series of operations executed for restoring one target such as a certain unit or load; N_K is the total number of steps in the restoration scheme, which is related to each restoration scheme; I_L^k, C^k, and R^k are the expected load restoration income, expected restoration cost, and security risk of step k, respectively, and they can be obtained by sampling and simulation of the restoration process of this step; $\boldsymbol{x}^k$ is the vector of system state variables of step k; $\boldsymbol{u}^k$ is the vector of control variables of step k, which includes the switching statuses of units, lines, and loads, and the adjustment of unit outputs; and $\boldsymbol{p}^k$ is the vector of disturbance variables of step k, which reflects the high-dimensional uncertainties of outage scenarios, external environment, and restoration processes.

For a deterministic restoration process of step k, the load restoration income I_L^k can be computed by (2), and the restoration cost C^k, including the electricity cost and preventive control cost during the restoration process, can be calculated by (3).

$$I_\mathrm{L}^k = \int_{t_s^k}^{t_\mathrm{e}} \alpha_\mathrm{L}^k(t)\Delta P_\mathrm{L}^k(t)\mathrm{d}t \quad (2)$$

$$C^k = \int_{t_s^k}^{t_\mathrm{e}} \mu_\mathrm{L}^k(t)\Delta P_\mathrm{L}^k(t)\mathrm{d}t + C_\mathrm{PC}^k \quad (3)$$

where t_s^k is the time when the target is restored based on step k; t_e is the preset end time of evaluation; C_PC^k is the cost of preventive control of step k; and $\alpha_\mathrm{L}^k(t)$, $\Delta P_\mathrm{L}^k(t)$, and $\mu_\mathrm{L}^k(t)$ are the restoration income per unit load, restored capacity, and electricity cost per unit restored load at time t based on step k, respectively. $\alpha_\mathrm{L}^k(t)$ and $\Delta P_\mathrm{L}^k(t)$ are influenced by the time duration of power outage [22], external environment [23], and user types [24]. For example, the cold load pick-up (CLPU) demand is an increased load in the restoration process due to the loss of load diversity, whose predict model can be established by data-driven [25] or model-driven [26] methods, and the load demand in the restoration process can be dynamically updated online. In addition, the restoration income per unit load and the load demand will be affected by load demand response (DR), which should also be modeled [27] and reflected to the time-varying load predict model.

The security risk R^k of step k includes the restoration operation risk and power grid operation risk, expressed as $R_\mathrm{O}^k = \sum_{m \in \Omega_\mathrm{O}^k} p_m^k e_m^k$ and $R_\mathrm{D}^k = \sum_{n \in \Omega_\mathrm{D}^k} p_n^k e_n^k$, respectively, where Ω_O^k and Ω_D^k are the fault sets of the restoration operation and an energized power grid, respectively; p_m^k and e_m^k are the probability and the optimal security control cost of the m^{th} restoration operation fault of step k, respectively; and p_n^k and e_n^k are the probability and the optimal security control cost of the n^{th} fault of the energized power grid of step k. The optimal security control cost includes emergency control cost and correction control cost.

2) Constraints

1) Steady-state constraints

$$P_{\mathrm{O},i}^k + P_{\mathrm{G},i}^k - P_{\mathrm{L},i}^k = V_i^k \sum_{j \in \Omega_\mathrm{N}^k} V_j^k (G_{ij}^k \cos\theta_{ij}^k + B_{ij}^k \sin\theta_{ij}^k) \quad \forall i \in \Omega_\mathrm{N}^k \quad (4)$$

$$Q_{\mathrm{O},i}^k + Q_{\mathrm{G},i}^k - Q_{\mathrm{L},i}^k = V_i^k \sum_{j \in \Omega_\mathrm{N}^k} V_j^k (G_{ij}^k \sin\theta_{ij}^k - B_{ij}^k \cos\theta_{ij}^k) \quad \forall i \in \Omega_\mathrm{N}^k \quad (5)$$

$$\underline{S}_{ij} \le S_{ij}^k \le \overline{S}_{ij} \quad \forall i,j \in \Omega_\mathrm{N}^k \quad (6)$$

$$\underline{V}_i \le V_i^k \le \overline{V}_i \quad \forall i \in \Omega_\mathrm{N}^k \quad (7)$$

$$\underline{P}_{\mathrm{G},i}^k \le P_{\mathrm{G},i}^k \le \overline{P}_{\mathrm{G},i}^k \quad \forall i \in \Omega_\mathrm{G}^k \quad (8)$$

$$\underline{Q}_{\mathrm{G},i}^k \le Q_{\mathrm{G},i}^k \le \overline{Q}_{\mathrm{G},i}^k \quad \forall i \in \Omega_\mathrm{G}^k \quad (9)$$

$$P_\mathrm{res}^{k-1} - \Delta P_\mathrm{L}^k \ge \gamma P_{\mathrm{G}\Sigma}^k \quad (10)$$

where Ω_N^k and Ω_G^k are the node set and generator set of the energized power grid at the end of step k, respectively; i and j represent the indices of nodes; $P_{\mathrm{O},i}^k$ and $Q_{\mathrm{O},i}^k$ are the active and reactive power that node i receives from the external

power system through tie-line at the end of step k, respectively; $P^k_{\mathrm{G},i}$ and $Q^k_{\mathrm{G},i}$ are the active and reactive power provided by the generator at node i at the end of step k, respectively; $P^k_{\mathrm{L},i}$ and $Q^k_{\mathrm{L},i}$ are the active and reactive power of the restored load at node i at the end of step k, respectively; V^k_i and V^k_j are the voltages at node i and node j, respectively; θ^k_{ij} is the difference of voltage phase angles between nodes i and j; G^k_{ij} and B^k_{ij} are the real and imaginary parts of impedance on line (i,j) at the end of step k, respectively; S^k_{ij}, $\underline{S}_{ij}$, and $\overline{S}_{ij}$ are the power transmission amount of line (i,j) and its lower and upper limits at the end of step k, respectively; $\underline{V}_i$ and $\overline{V}_i$ are the lower and upper limits of voltage at node i, respectively; $\underline{P}^k_{\mathrm{G},i}$, $\overline{P}^k_{\mathrm{G},i}$, $\underline{Q}^k_{\mathrm{G},i}$, and $\overline{Q}^k_{\mathrm{G},i}$ are the lower and upper limits of active power output and reactive power output of generator at node i at the end of step k, respectively; P^{k-1}_{res} is the rotating reserve capacity of energized power grid at the end of step $k-1$; ΔP^k_{L} is the active power of the incrementally restored loads of step k; γ is the spinning reserve factor of the energized power grid; and $P^k_{\mathrm{G}\Sigma}$ is the total capacity of the rated power supplied by the available generators in the energized power grid at the initial time of step k.

For three-phase unbalanced distribution systems, the steady-state constraints of each phase should be considered [28]. The constraints of start-up power demand, climbing rate, and cold and hot start-up time limits for thermal power units should also be considered [23]. The constraints of the number of charging and discharging times and the state of charge of energy storage devices should also be considered.

2) Transient constraints

In order to avoid the transient impact during load pickup, the constraint of active power of single-step load restoration is expressed as:

$$\Delta P^k_{\mathrm{L,step}} \le \zeta P^k_{\mathrm{G}\Sigma} \tag{11}$$

where $\Delta P^k_{\mathrm{L,step}}$ is the maximum active power of single-step load restoration at step k; and ζ is the ratio coefficient of the $\Delta P^k_{\mathrm{L,step}}$ to $P^k_{\mathrm{G}\Sigma}$.

After the restoration schemes are generated, it is necessary to verify the transient voltage and frequency security of the schemes through numerical simulations. In addition, when multiple power sources are networked, the inertia constraint, together with the transient voltage and current constraints when changing the power source control-mode, should also be considered.

3) Topology constraint

For the energized power grid, to ensure that it is operated in tree topology, its topology at the end of each step should be a connected graph and satisfy (12).

$$\sum_{i \in \Omega^k_{\mathrm{N}}} s^k_{\mathrm{N},i} - \sum_{(i,j) \in \Omega^k_{\mathrm{B}}} s^k_{\mathrm{B},ij} = \sum_{g \in \Omega^k_{\mathrm{GBS}}} s^k_{\mathrm{G},g} \quad \forall j \in \Omega^k_{\mathrm{N}} \tag{12}$$

where Ω^k_{B} is the set of branch lines in the energized power grid; Ω^k_{GBS} is the node subset of TDBs and black start DGs in the energized power grid; $s^k_{\mathrm{B},ij}$ denotes the energization status of line (i,j) at the end of step k, and $s^k_{\mathrm{B},ij}$=1 when line (i,j) is energized and $s^k_{\mathrm{B},ij}=0$ when line (i,j) is de-energized; $s^k_{\mathrm{N},i}$ denotes the energization status of node i at the end of step k, and $s^k_{\mathrm{N},i}=1$ when node i is energized and $s^k_{\mathrm{N},i}=0$ when node i is de-energized; and $s^k_{\mathrm{G},g}$ denotes the energization status of unit g at the end of step k, and $s^k_{\mathrm{G},g}=1$ when unit g is energized and $s^k_{\mathrm{G},g}=0$ when unit g is de-energized. In this paper, only one TDB or black-start DG is assumed to exist in the energized power grid, i.e., (12) can be used for the systems with multiple substation nodes and black-start DGs to form multiple isolated subsystems. However, the spinning reserve constraints and frequency response rate (FRR) constraints must be adapted accordingly.

III. General Framework of Proposed DRDSS

The general framework of the proposed DRDSS is presented in Fig. 1. The proposed DRDSS exchanges real-time information with distribution management system (DMS) and wide-area monitoring analysis protection-control (WARMAP) system [29], monitors the execution results of restoration control measures, and adaptively adjusts the restoration scheme to provide restoration decision-making support to the operators. The framework of DRDSS comprises two parts, i.e., the information processing part and the analysis and decision-making part. The latter part adopts a two-layer optimization framework, where the upper layer conducts the global coordination, and the lower layer conducts the partition optimization. The restoration operations are accomplished in an open-loop, closed-loop, or mixed manner. In the open-loop manner, the system operator confirms the restoration scheme and issues the restoration instructions. In the closed-loop manner, the proposed DRDSS issues the restoration instructions to the actuators directly. In the mixed manner, the restoration instructions are issued to the actuators automatically and the system operator can adjust the instructions when necessary. The proposed DRDSS also consists of on-line operation mode and training simulation mode, and the configuration for the two modes is presented in [21].

A. Information Interface

The information interface enables the DRDSS to interact with DMS, WARMAP, and other dispatching automation systems. This information interface obtains the data required for the restoration decision-making from the distribution system such as operation information of the distribution system, power support information of the adjacent external distribution systems, and warning information regarding external disasters such as equipment failure probability, etc. In addition, it also enables the DRDSS to interact with the energy management system (EMS), WARMAP, and other automation systems of related transmission systems to obtain information from transmission system side. This information includes the maximum and actual values of the power delivery from transmission system to distribution systems through TDBs, the connectivity relationship of TDBs at transmission system side, and the power demand of transmission system from distribution systems. Moreover, the information interface can also be used to send the information to the related transmission system such as the load demand of the distribution system, the maximum power that distribution system can provide to the transmission system, etc. In the decision-making and implementation processes of restoration, all this information will be dynamically updated from DMS, EMS, WARMAP, and other related systems.

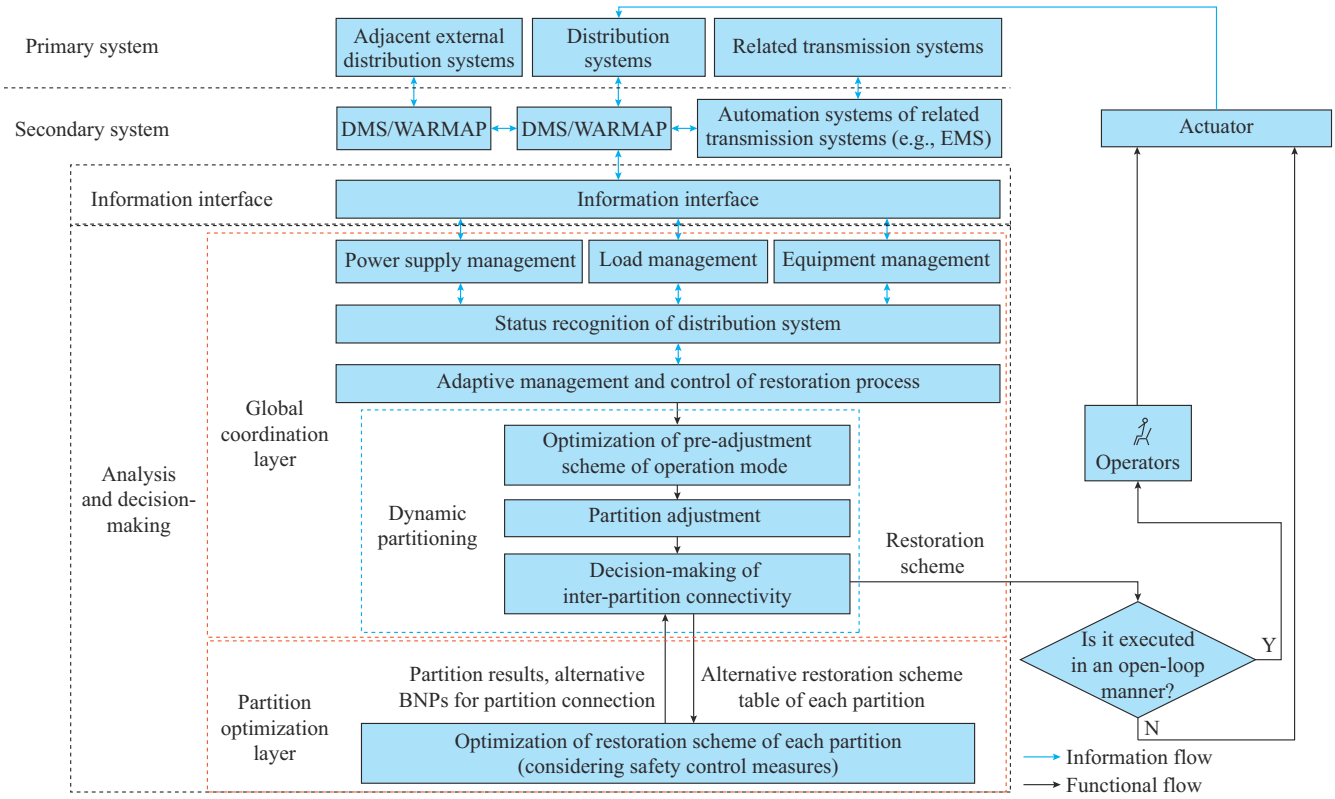

Fig. 1. Framework of proposed DRDSS.

B. Global Coordination

The modules of management and system status recognition in the global coordination layer are used to analyze the outage scenarios based on the latest information. The adaptive management and control module of restoration process monitors the restoration process of each partition based on the restoration schemes recommended by the dynamic partitioning module, and adaptively sends the scheme switching or re-optimizing instructions to the dynamic partitioning module. The dynamic partitioning module, including pre-adjustment scheme optimization of operation mode, partition adjustment, and decision-making of inter-partition connectivity, is responsible for coordinating the optimization process of all the partitions. It sends the partitioning result and alternative boundary node pairs (BNPs) for inter-partition connectivity to the partition optimization layer. Afterwards, the dynamic partitioning module obtains the table of alternative restoration scheme for each partition dynamically uploaded by the partition optimization layer, performs connectivity decision-making, and recommends the restoration schemes of all partitions.

1) Real-time Information Management

The equipment management module analyzes the operation status, loading condition, restoration progress, measurement and control capabilities, fault probability, and other information of the equipment in distribution system. For the equipment with poor measurement and control capabilities, its parameters can be supplemented and dispatched by operators. In order to coordinate the restoration resources from the global perspective, it is necessary to shut down the distributed automatic power supply restoration equipment or systems that are based on local information in a timely manner such as automatic reclosing device, standby automatic switching device, and feeder automation system.

The power supply management module manages various intermittent or non-intermittent available power supply sources in the distribution system, including power support from the adjacent external transmission and distribution systems, black-start units in the distribution system, and the energized power grids that operate independently after an outage. The energized distribution power grids may have the power support from the external transmission system, or from the distribution system itself only. The power supply information includes operation status, available power capacity, start-up conditions (start-up power requirement and time consumption), and networking ability (feasible control modes and their switching capabilities). The available power capacity is embodied as the power output curve of the available power supplies, including the power delivery plan curve from the transmission system to the distribution system at each TDB, and the curves of the maximum active power capacity increment of the restored or under-restoration distribution power supplies, in which the power capacity curves of intermittent power supplies in the distribution system need to be predicted.

The load management module is used to analyze the load restoration progress at each load node. It manages the load demand information of both the distribution system and the adjacent external transmission and distribution systems. The load information of distribution system includes the power

demand curves and the curves of restoration income per unit load of each phase at each load node, where the load can be the restored, under-restoration, or to-be-restored load.

2) Status Recognition

The status recognition module of distribution system analyzes the status of power plants and substations in the distribution system, and identifies both the isolated and non-isolated outage regions. The isolated outage region refers to the outage region where there is no recoverable path between the node that belongs to this region and any energized node in the distribution system. Please note that the nodes in the distribution system include T-type nodes and other nodes including TDBs, generator terminal nodes, tie-line nodes, and load nodes. It is possible to change an isolated outage region to a non-isolated outage region by using mobile emergency power supply or equipment repair. The power supplying scope of the energized power grid is determined by considering the current maximum capacities of all power supplies connected to the energized power grid, the number of switch operations on the power delivery path, and other correlative factors. The maximum capacity is related to the maximum value of power delivery plan from the transmission system to the distribution system at TDB, and the rated capacity of non-intermittent power supply in the distribution system, etc. In order to effectively guide the transmission system to send the power to the distribution system during the collaborative restoration of transmission and distribution systems, the module sends information, including the power demand curve and the curve of restoration income per unit to-be-restored load in the distribution system at TDBs, to the relevant transmission system through the information interface.

3) Adaptive Management and Control of Restoration Process

The flowchart of adaptive management and control of restoration process is shown in Fig. 2. When a power outage occurs, this module initiates the first-time optimization of the restoration schemes. In the restoration process, this module adaptively determines whether it is necessary to switch the current restoration scheme to a sub-optimal scheme or to re-optimize the schemes according to the actual execution process of each partition. If the module detects that the partition is undergoing or is planned to undergo security control, the restoration operations of the relevant partition are suspended. After the security control is completed, the module decides whether to resume the implementation of the original restoration scheme according to the real-time operation conditions of the power grid.

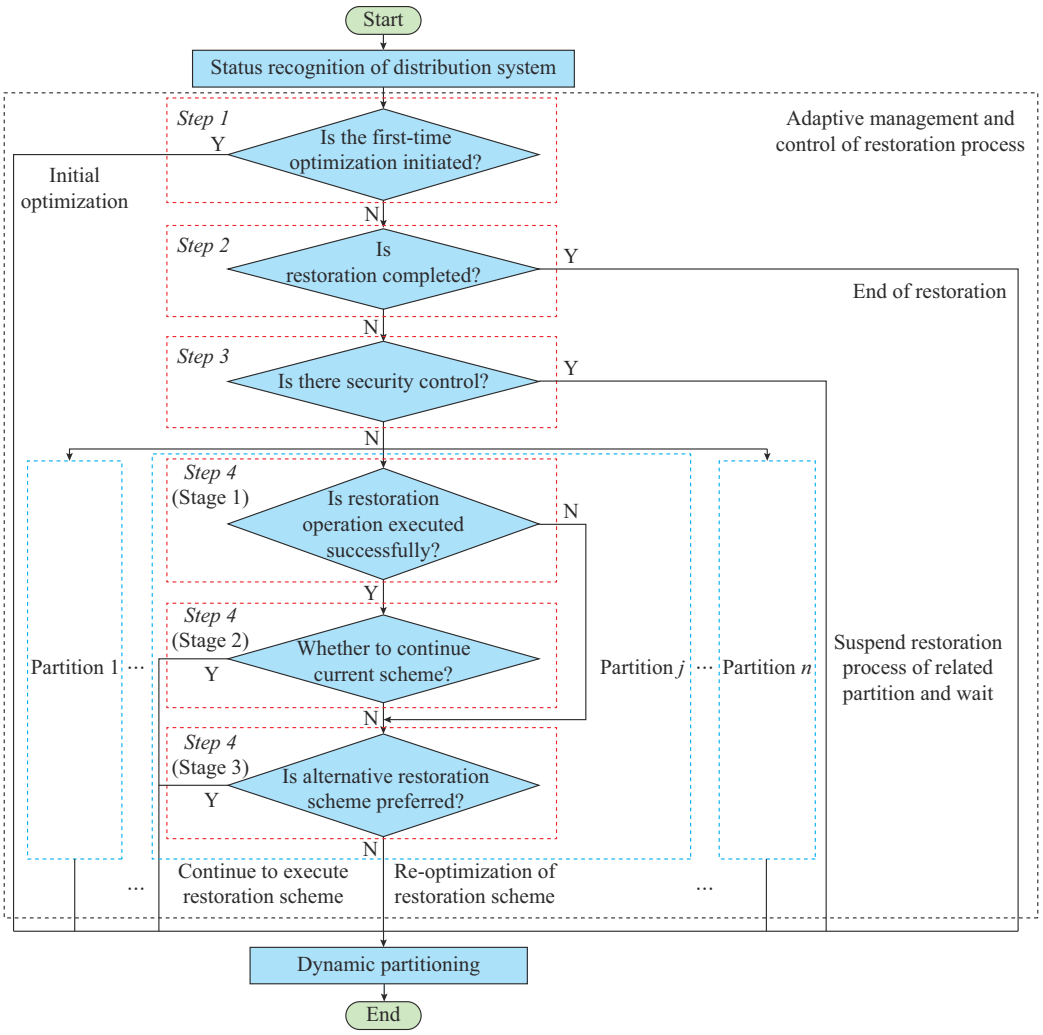

Fig. 2. Flowchart of adaptive management and control of restoration process.

The steps of the adaptive management and control module are as follows.

Step 1: determine whether to initiate the first-time optimization of the restoration schemes. If the optimization is initiated, send the first-time optimization instruction to the dynamic partitioning module; otherwise, proceed to *Step 2*.

Step 2: identify whether the restoration of the distribution system is completed. If it is completed, the module sends the restoration end signal to the dynamic partitioning module; otherwise, proceed to *Step 3*.

Step 3: for the partitions that are undergoing or are planned to undergo security control, suspend the restoration operations of related partitions, and send an instruction of waiting for the end of security control to the dynamic partitioning module. For the partitions where the security control is completed or there is no security control, proceed to *Step 4*.

Step 4: perform the adaptive management and control of the restoration process of each partition. This step is further divided into the following stages.

1) Stage 1: determine whether the current restoration operation is executed successfully. If it is executed successfully, proceed to Stage 2; otherwise, proceed to Stage 3. If an equipment is identified as the permanent fault, its status is recorded as unrecoverable until the fault is eliminated.

2) Stage 2: determine whether to continue the current scheme or not. If yes, send a continue execution instruction to the dynamic partitioning module; otherwise, proceed to Stage 3. Considering the influence of uncertainties in the restoration process and external environment, the following conditions should be met at the same time when continuing the current scheme: ① there are subsequent operations in the current scheme and the related equipment can still be restored; ② there is no new outage node in the energized power grid such as unit shut-down and load shedding caused by an emergency or correction control; ③ compared with the time when the current scheme is generated, the variations in both the restoration operation risk and energized power grid operation risk do not exceed the predefined thresholds; ④ the maximum difference between the estimated restoration income of the current restoration target and that of other remaining-to-be-restored targets in the partition does not exceed the predefined threshold; ⑤ the difference of the power delivery plan and the actual power delivered between transmission and distribution systems at TDB does not exceed the preset threshold; and ⑥ the maximum adjustment amount of the power delivery plan curve at TDB between transmission and distribution systems does not exceed the preset threshold.

3) Stage 3: identify if there is a feasible sub-optimal alternative restoration scheme. If yes, send an instruction of switching to the alternative scheme and continue the restoration process to the dynamic partitioning module; otherwise, send a re-optimization instruction to the dynamic partitioning module.

When the transmission and distribution systems are restored collaboratively, this module exchanges the information with the related transmission system through the information interface module. The module not only receives the information such as the transmission system partition that each TDB belongs to and the power delivery plan curves between transmission and distribution systems, but also transmits the information such as the end of actual restoration operation of distribution system to the EMS of the relevant transmission system.

4) Dynamic Partitioning

The dynamic partitioning module receives the instructions issued by the adaptive management and control module of the restoration process. Based on the information of the outage scenario, the restoration process, and the power delivery plan curve at TDB between transmission and distribution systems, this module optimizes the pre-adjustment scheme of operation mode for the energized power grids and the partitions, and makes a decision regarding the inter-partition connectivity.

If the adaptive management and control module of the restoration process issues the first-time optimization or re-optimization instructions, the dynamic partitioning module optimizes the pre-adjustment scheme of operation mode and determines the initial partitions (or adjusts the partitions), makes recommendations on the inter-partition connectivity, and sends the partitioning result and alternative BNPs for the inter-partition connectivity to the partition optimization layer. After the partition optimization layer uploads the table of alternative restoration scheme of each partition, the optimal restoration scheme of each partition, together with the inter-partition connectivity schemes, is optimized and recommended. Please note that, before adjusting the partitions, it is necessary to mark the original partition and status of each device. The status can be running, under-restoration, scheduled-to-be-restored, remaining-to-be-restored, or unrecoverable. The under-restoration devices can no longer change their partition attribution, and the devices in scheduled-to-be-restored status can be restored according to the current schemes, whereas the devices in remaining-to-be-restored status require re-optimization for restoration schemes.

If the adaptive management and control module of the restoration process issues the instruction of waiting for the end of security control, the restoration process of the related partition is suspended.

If the adaptive management and control module of the restoration process issues the continue execution instruction, the dynamic partitioning module continues to recommend the current or alternative schemes and simultaneously receives the table of alternative restoration scheme of each partition expanded dynamically by the partition optimization layer.

If the adaptive management and control module of the restoration process sends the distribution system restoration end signal, the dynamic partitioning module stops the optimization and recommendation of restoration schemes and provides the system operators with relevant information.

1) Optimization of pre-adjustment scheme of operation mode

The optimization submodule for pre-adjustment scheme of operation mode pre-adjusts the operation mode of the energized power grid through load transfer, which provides a more reasonable decision-making space for the subsequent

dynamic partitioning and partition optimization, thus improving the global restoration benefits. Distribution systems usually operate in a radial structure, so the energized distribution grid is generally regarded as a tree with TDB or the power supply that has sufficient frequency/voltage control capability and the maximum power generation capacity as its root with loads or switches as its leaves [30]. In this paper, it is defined as a power-supplied tree. A sample of energized power grid pre-adjustment in a power outage scenario of a distribution system is shown in Fig. 3, where P_{TDB1} and P_{TDB2} are the power delivery from TDB_1 and TDB_2, respectively. The power-supplied tree with TDB_1 as its root has a heavy-loaded path TDB_1-1, which makes it impossible to supply power to the remaining-to-be-restored loads connected to either the power-supplied subtree with node 1 as its root or the power outage nodes such as 6 and 30. By closing path 9-25 and opening path 3-8, or closing paths 33-5, 5-6, 6-7 and opening path 3-8, the power-supplied subtree with node 8 as its root can be transferred to either the energized power grid supplied by TDB_2 with sufficient power or the subtree of the energized power grid itself that is light-loaded. This is conducive to improving the overall restoration income of all the available power supplies in the distribution system.

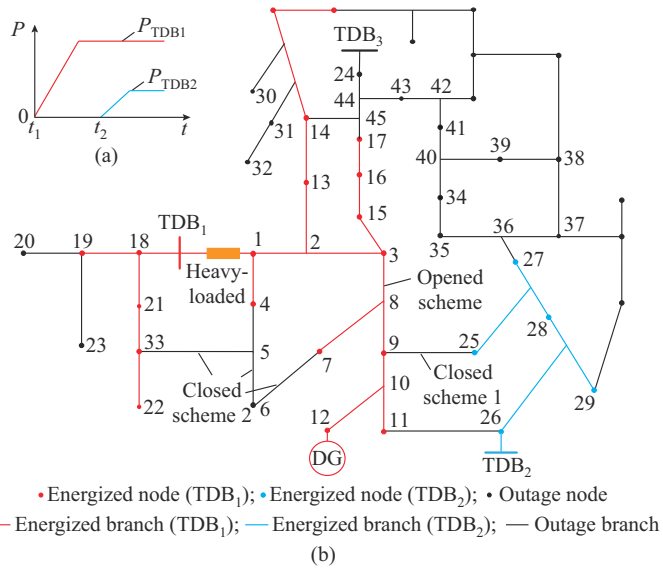

Fig. 3. A sample of energized power grid pre-adjustment in a power outage scenario of a distribution system. (a) Power delivery plan from transmission system. (b) Schematic diagram of energized power grid pre-adjustment.

In this paper, the pre-adjustment of operation mode is achieved by optimizing the energized load transfer scheme. Thus, the set of scenarios including the initial scenario and the scenarios derived from the pre-adjustment scheme of operation mode is obtained. According to whether there is a load outage in the process of energized load transfer, the energized load transfer can be divided into two categories, i.e., hot-transfer and cold-transfer. The hot-transfer means that the energized power grids are first connected at a switch, and then opened at an appropriate switch to transfer the loads without causing power outage. The connection between two energized distribution power grids supplied by different TDBs that belong to the same transmission system partition is a closed-loop operation. Besides, the cold-transfer means that the loads to be transferred are first disconnected from the energized power grid, and then connected to another energized power grid through a feasible path. The load outage loss is computed using (2). It is notable that the hot-transfer should be given priority if the following conditions are met at the same time: ① the phase sequence of both ends of the switch to be closed is consistent; and ② the maximum voltage difference and phase angle difference of both ends of the switch to be closed do not exceed the preset thresholds [31]. If DG exists in the subtree to be transferred, the networking conditions of multiple power supplies should be met during and after the transfer [32], including a feasible coordinated voltage/frequency control mode among power supplies, feasible protection configurations, and operation modes with security verified.

The flowchart for the optimization of energized load transfer scheme is presented in Fig. 4. Its major steps are presented as below.

Step 1: determine the power supplying scope of each energized power grid, evaluate the energized load transfer demand index J of each energized power grid according to (13), and add the energized power grids whose J are greater than the preset threshold value $\varepsilon_{\mathrm{J}}(\varepsilon_{\mathrm{J}}>0)$ to $\Omega_{\mathrm{TA}}=\{TA_i|i=1,2,\ldots,N_{\mathrm{TA}}\}$, where Ω_{TA} is the set of energized power grids which are waiting for load transfer decision-making.

$$J=\sum_{j=1}^{N_{\mathrm{J}}}\int_{t_j}^{t_{\mathrm{e}}}\alpha_{\mathrm{L},j}(t)\left(\Delta P_{\mathrm{L},j}^{\mathrm{need}}(t)-\Delta P_{\mathrm{L},j}^{\mathrm{ava}}(t)\right)\mathrm{d}t \tag{13}$$

where N_{J} is the total number of load nodes to be restored within the power supplying scope of the energized power grid, including both the outage load nodes and the energized load nodes with remaining-to-be-restored loads; j is the serial number of the load node to be restored within the power supplying scope of the energized power grid; t_j is the estimated restored time of load node j, which is evaluated based on the shortest path; t_j-t_{e} is the evaluation period; $\alpha_{\mathrm{L},j}(t)$ and $\Delta P_{\mathrm{L},j}^{\mathrm{need}}(t)$ are the restoration income curve per unit load and capacity curve of the load to be restored at load node j, respectively; and $\Delta P_{\mathrm{L},j}^{\mathrm{ava}}(t)$ is the increment power that load node j currently obtains from the energized power grid. To determine the increment power allocation on the load nodes, all the load nodes in the power supplying scope of the energized power grid are sorted in descending order based on the restoration income per unit load of the loads to be restored, and then the current available power of the energized power grid is allocated to the load nodes by order on the premise of meeting the security constraints which can be satisfied by restoring double circuit lines and reactive power compensation devices. Please note that $\Delta P_{\mathrm{L},j}^{\mathrm{ava}}(t)\le\Delta P_{\mathrm{L},j}^{\mathrm{need}}(t)$ and $J\ge 0$. The large J of the energized power grid indicates that it is unable to meet the load restoration demand within its own power supplying scope in the current operation mode of the distribution system. Thus, there is a need for operation mode adjustment and optimization of the energized power grid.

Step 2: if Ω_{TA} is an empty set, end this process; otherwise, proceed to *Step 3*.

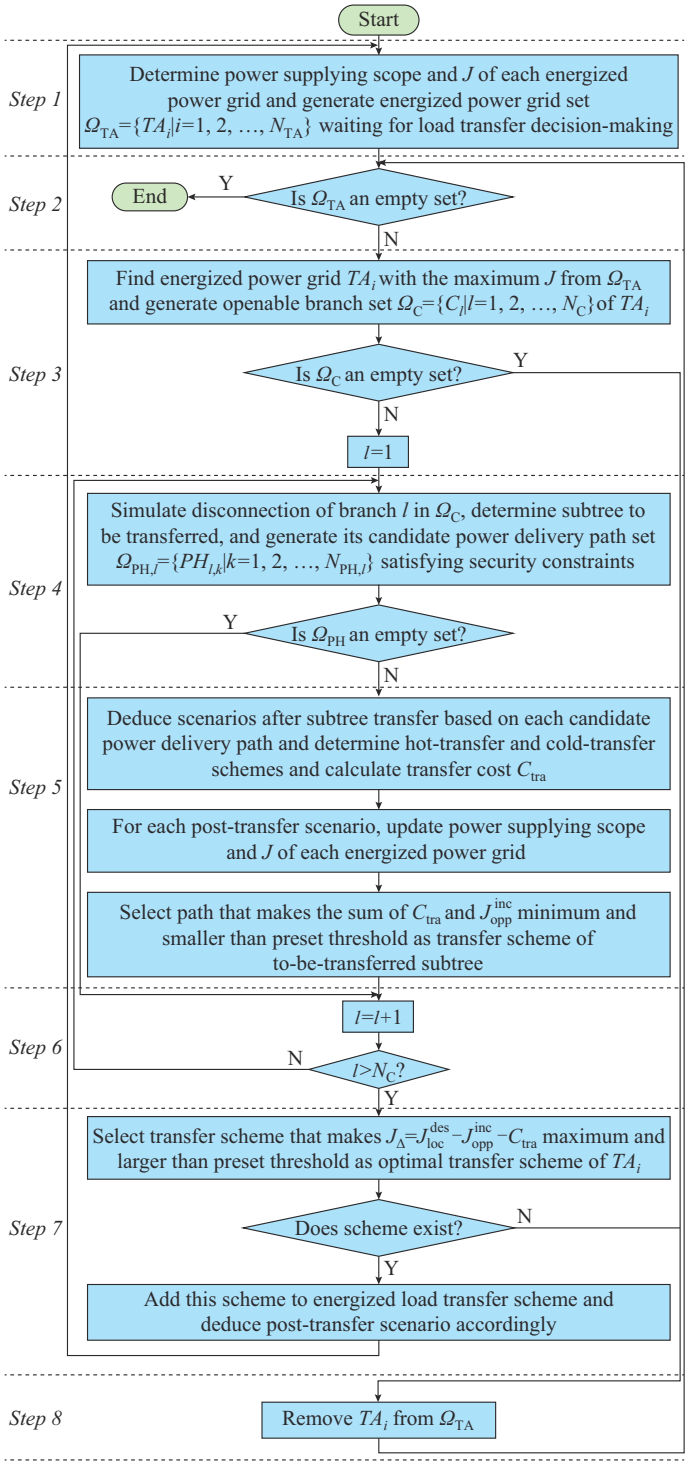

Fig. 4. Flowchart for optimization of energized load transfer scheme.

Step 3: find the energized power grid $TA_i (1 \le i \le N_{TA})$ with the maximum J from set Ω_{TA}. Denote TA_i as a power-supplied tree, and generate the openable branch set $\Omega_C = \{C_l | l = 1, 2, \ldots, N_C\}$ of TA_i. If Ω_C is an empty set, proceed to *Step 8*; otherwise, assume $l = 1$, and proceed to *Step 4*.

Step 4: simulate the disconnection of branch l in Ω_C, and the power-supplied subtree with child node of branch l as its root is to-be-transferred. Furthermore, for the to-be-transferred subtree, generate the set of candidate power delivery paths $\Omega_{PH,l} = \{PH_{l,k} | k = 1, 2, \ldots, N_{PH,l}\}$ that can provide power supply to the subtree and satisfy the security constraints, and the set of energized power grids $\Omega_{CA} = \{CA_k | k = 1, 2, \ldots, N_{PH,l}\}$ that can supply power to the subtree. Now, if $\Omega_{PH,l}$ is an empty set, proceed to *Step 6*; otherwise, proceed to *Step 5*. The candidate power delivery paths only receive power supports from the nodes of either the same voltage level or the higher voltage level. The available power capacity of the energized power grid in Ω_{CA} should be greater than the current total load of the subtree to be transferred; otherwise, it is necessary to consider the load shedding of the to-be-transferred subtree or the energized power grids in Ω_{CA}.

Step 5: based on each candidate power delivery path, the scenarios after the to-be-transferred subtree transfer are obtained through simulation and deduction, and the hot-transfer or cold-transfer schemes are determined accordingly. Please note that the transfer cost only considers the load outage loss in the cold-transfer process. For each scenario after the load transfer, the power supplying scope and J of each energized power grid are updated. The path that makes the sum of C_{tra} and J_{opp}^{inc} minimum and smaller than the preset threshold is selected as the transfer scheme of the to-be-transferred subtree, where C_{tra} is the cost of load transfer; and J_{opp}^{inc} is the increment of J of the energized power grid, to which the load is transferred. If this path is not unique, the path whose opposite-end energized power grid has the smallest J is selected.

Step 6: set $l = l + 1$. If $l > N_C$, proceed to *Step 7*; otherwise, go back to *Step 4*.

Step 7: from the transfer schemes of all the subtrees of TA_i, the transfer scheme that makes $J_\Delta = J_{loc}^{des} - J_{opp}^{inc} - C_{tra}$ maximum and larger than the preset threshold is selected as the optimal transfer scheme of TA_i, where J_{loc}^{des} is the descent of J of the energized power grid in Ω_{TA} after the subtree is transferred out. If this scheme exists, add it to the transfer scheme of energized load, then deduce the post-transfer scenario accordingly, and go back to *Step 1*; otherwise, if the scheme does not exist, proceed to *Step 8*.

Step 8: remove TA_i from Ω_{TA}, and go back to *Step 2*.

The aforementioned process can be used to obtain a transfer scheme of the energized load. By relaxing the optimization conditions of transfer schemes considered in *Step 7*, the transfer schemes of several subtrees of TA_i can be selected, deduced, and optimized according to the aforementioned process. Thus, there will be several candidate transfer schemes of energized load, which can generate a set of expected outage scenarios Ω_P, including the real-time outage scenario $\Omega_P(1)$ and the pre-adjusted scenarios $\Omega_P(z)$ $(z = 2, 3, \ldots, N_Z)$ generated from $\Omega_P(1)$ according to each candidate energized load transfer scheme, where N_Z is the total number of outage scenarios in Ω_P.

2) Partition adjustment

This submodule determines or adjusts the partitions based on scenarios in Ω_P one by one to determine the optimal pre-adjustment scheme of operation mode and the corresponding partitioning result. The main steps of this submodule are presented as follows.

Step 1: determine the power supplying scope of each energized power grid and set the partition of each energized power grid accordingly. If there is an overlapping area between

the partitions, i.e., the nodes to be restored in this area are repeatedly divided into two or more partitions, proceed to *Step 2*; otherwise, proceed to *Step 3*.

Step 2: modify the scope of each partition according to the following stages to eliminate the overlap between partitions.

① Stage 1: update the available power curve of each partition and generate the available power allocation scheme at each load node of each partition. The available power in each partition is allocated to each load node according to the restoration income per unit remaining-to-be-restored load at each load node, including energized and outage load nodes.

② Stage 2: the estimated restoration income that each load node generates when receiving power through different paths is evaluated. First, aiming at load node i which needs to be restored and obtains power allocation, search the path set $\Omega_{\mathrm{H},i,j}=\{H_{i,j,l}|l=1,2,\ldots,N_{\mathrm{H},i,j}\}$ of load node i that receives the power from partition j considering the number of required intermediate nodes, where $N_{\mathrm{H},i,j}$ is the total number of paths through which the load node i receives power from partition j. Then, the restoration value $W_{i,j,l}$ of path $H_{i,j,l}$ is evaluated according to (14).

$$W_{i,j,l}=I_{i,j,l}/N_{\mathrm{H},i,j} \tag{14}$$

where $I_{i,j,l}$ is the estimated restoration income generated by restoring the load at load node i according to path $H_{i,j,l}$. This is evaluated by using (2) based on the power allocated by partition j at load node i.

③ Stage 3: Ω_{Br} is assumed as the set of outage branches in all the current overlapping areas. The restoration value of each outage branch in Ω_{Br} is calculated, specifically, the restoration value $W_{\mathrm{Br},m}$ of outage branch m is obtained by (15).

$$W_{\mathrm{Br},m}=\sum_{i=1}^{N_{\mathrm{B}}}\sum_{j=1}^{N_{\mathrm{P}}}\sum_{l=1}^{N_{\mathrm{H},i,j}}u_{i,j,l,m}W_{i,j,l} \tag{15}$$

where N_{B} is the total number of load nodes that obtain power allocation in the current scenario; N_{P} is the total number of partitions in the current scenario; and $u_{i,j,l,m}$ is the identification of whether the l^{th} path $H_{i,j,l}$ of node i that receives power from partition j passes through the outage branch m.

④ Stage 4: based on the current outage scenario, the outage branch with the smallest restoration value in Ω_{Br} is removed by simulation. If there are multiple outage branches with small restoration values, the branch removal should avoid adding new outage nodes that do not belong to any partition. If it is unable to avoid this, then the branch whose removal causes the smallest decrease in the sum of the estimated restoration income of each partition should be removed.

⑤ Stage 5: update the area of each partition. If there are still overlapping areas between the partitions, go back to Stage 1; otherwise, go to *Step 3*.

Step 3: generate the partitioning result and calculate I_{P}, which is the sum of the maximum estimated restoration incomes of all partitions, according to (2).

Step 1-*Step 3* are repeated for each outage scenario in Ω_{P} to obtain the partitioning results and the corresponding estimated restoration income vector $\boldsymbol{I}_{\mathrm{P}}$. For partitioning results when $z=2,3,\ldots,N_{\mathrm{Z}}$, if there is a partitioning result that satisfies $\max\{\boldsymbol{I}_{\mathrm{P}}(z)-\boldsymbol{I}_{\mathrm{P}}(1)\}/\boldsymbol{I}_{\mathrm{P}}(1)>\varepsilon_{\mathrm{P}}$, where ε_{P} denotes the preset threshold, then the partitioning result with the largest $\boldsymbol{I}_{\mathrm{P}}(z)-\boldsymbol{I}_{\mathrm{P}}(1)$ is taken as the optimal one, and is sent to the decision-making submodule of inter-partition connectivity along with its corresponding outage scenario; otherwise, there is no other suitable way to pre-adjust the current operation mode, and the partitioning result of real-time outage scenario $\Omega_{\mathrm{P}}(1)$ is sent to the decision-making submodule of inter-partition connectivity.

Taking Fig. 5(a) as an example, there are two radial energized power grids with TDB_1 and TDB_2 as their roots, respectively. The power delivery plan from transmission system is the same as shown in Fig. 3(a). The power supplying scope of each energized power grid is presented by colored area in Fig. 5(a), corresponding to two partitions. There are two overlapping areas between the partitions. So, it is necessary to further revise the scope of the partition. The available power allocation scheme of the partition, where TDB_1 is located, includes nodes 34 and 37. Similarly, the available power allocation scheme of the partition, where TDB_2 is located, includes nodes 6, 34, and 37. The available power delivery paths of nodes 6 and 34 are presented by the arrows in Fig. 5(a). According to the restoration value of each outage branch, the partition de-overlapping scheme of removing outage branches ① to ③ is obtained through the aforementioned steps, and the outage branch removals are simulated sequentially. The partitioning result is shown in Fig. 5(b).

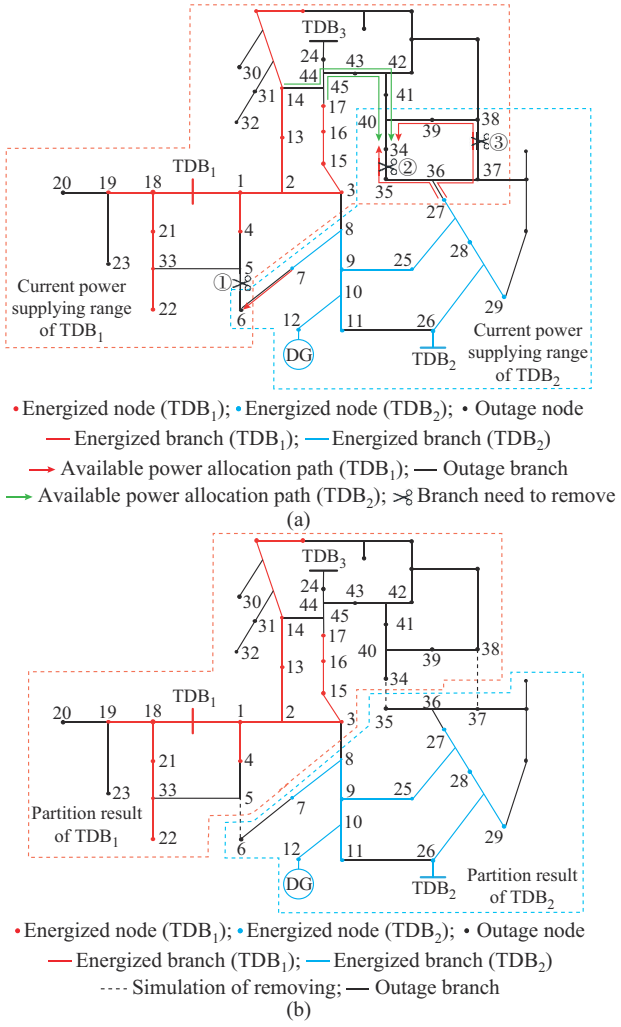

Fig. 5. Schematic diagram of partitioning optimization. (a) Process of partition de-overlapping. (b) Partitioning result.

After obtaining the deterministic partitioning result, the decision-making of inter-partition connectivity and partition optimization are performed successively. The global expected net income of the restoration schemes of all the partitions is also calculated. It is notable that if some other partitioning strategies are adopted, the partitioning result may be changed. However, for each type of partitioning result, its global expected net income can still be calculated according to the same decision-making process, and the optimal partitioning result will be determined.

3) Decision-making of inter-partition connectivity

Based on the partitioning result, the decision-making submodule of inter-partition connectivity recommends alternative BNPs for inter-partition connectivity and modifies them dynamically in the restoration process. After obtaining the table of alternative restoration scheme of each partition uploaded by the partition optimization layer, which will be introduced in Section III-C, the submodule checks the partition connecting conditions including the conditions of inter-partition synchronization, and the security and stability conditions of connected partitions. Afterwards, it optimizes the inter-partition connectivity schemes according to the method in [21], which includes the schemes of the two partitions delivering power to restore their boundary nodes and the scheme of the two boundary nodes being connected with a branch.

C. Optimization of Restoration Scheme for Each Partition

The partition optimization layer optimizes the table of the alternative restoration scheme for each partition in parallel, and sends the result to the decision-making submodule of inter-partition connectivity. Following the idea presented in [21] regarding the unified sorting of unit nodes and load nodes, the generation of scheme tree based on the scheme deduction, and scheme sorting index of the expected net income per unit of power consumption, we perform screening and unified sorting on the restoration targets, optimize the restoration path of each restoration target, and generate the table of alternative restoration scheme of the partition with a certain search breadth. During the restoration scheme optimization, the number of different restoration targets starting from the same actual outage scenario or simulated outage scenario is limited by search breadth. A new simulated outage scenario is generated by the deduction of any one-step restoration scheme in the table of alternative restoration scheme. By repeating the aforementioned breadth optimization process, the table of alternative restoration scheme of the partition with a certain search depth is obtained.

The restoration targets refer to the remaining-to-be-restored units and substation nodes. During the restoration target screening, in addition to the factors of spinning reserve capacity constraints, transient frequency and voltage constraints, hot-start and cold-start requirements of units, etc., it is also necessary to consider the factors such as the networking conditions of power supplies and the grid connecting conditions of intermittent power supplies. During the restoration target sorting, the restoration income I_G of remaining-to-be-restored unit that has start-up power demand is evaluated by (16). The restoration income I_B of remaining-to-be-restored substation node is evaluated by (17).

$$I_G = e^{-\min\{\eta_{sys},\eta_{part}\}}(\beta_{GP} I_{GP} - C_{GP}) \tag{16}$$

$$I_B = (1 - e^{-\min\{\eta_{sys},\eta_{part}\}})(\beta_{BL} I_{BL} - C_{BL}) + e^{-\min\{\eta_{sys},\eta_{part}\}} \beta_{GN} I_{GN} \tag{17}$$

where η_{sys} and η_{part} are the satisfaction rates of the power system restoration demand and partition restoration demand, respectively, which are the ratios of the sum of capacities of spinning reserve and the under-restoration units to the capacity of remaining-to-be-restored loads; β_{GP} ($0<\beta_{GP}\le 1$) is the conversion coefficient of the indirect restoration income of a unit, which indicates the delay effect of time consumption of the restoration process after the unit is connected to the power grid on the restoration income; I_{GP} is the estimated load restoration income generated after the unit is connected to the power grid, which is calculated using (2), where the estimated load restoration income of non-intermittent power supply is calculated according to the rated power of the unit, whereas the estimated load restoration income of intermittent power supply is calculated according to the lower limit of the unit's predicted output curve; C_{GP} is the cost of restoring a unit; β_{BL} ($0<\beta_{BL}\le 1$) is the conversion coefficient of the node restoration income; I_{BL} is the estimated load restoration income of a substation node, i.e., the maximum load restoration income calculated by (2), supposing all the available power of the partition is used to restore the loads at the substation node and the loads within its partition; C_{BL} is the restoration cost of the loads at the substation node; β_{GN} ($0<\beta_{GN}\le 1$) is the conversion coefficient of the indirect restoration income of a unit without start-up power demand at the substation node; and I_{GN} is the estimated load restoration income that can be obtained after the unit is restored and connected to the energized power grid. For a remaining-to-be-restored node that is connected with unit, if the unit is allocated to the partition that cannot satisfy the networking conditions of the unit, then the unit cannot be restored and therefore its estimated restoration income is assigned to zero; otherwise, the unit can be restored and its estimated restoration income is the estimated load restoration income that can be generated after the unit obtains the start-up power and connects to the energized power grid.

A variety of security events can occur in the restoration process of distribution system with high-dimensional uncertainties. The feasibility, security, and economy of the restoration scheme will be affected if the pre-adjustment ability of operation mode before restoration operation or the demand of security control after restoration operation is neglected. In this paper, the effects of preventive control, emergency control, and correction control are considered during the optimization of the restoration path, and the decision-making space of restoration schemes is expanded by operation mode pre-adjustment of the energized power grid in advance. In addition, the costs of emergency control and correction control possibly introduced by the operation of each restoration scheme are considered in the evaluation of the security risks and net incomes of the restoration schemes. When optimizing the restoration scheme of step k, for a certain restoration path of the restoration target, the security verification and

evaluation according to the following steps are performed.

Step 1: based on the real-time scenario, the security verification for the restoration operation is performed. If a restoration operation fails to pass the security verification, its optimal preventive control measures and costs [33] are optimized to enable the restoration operation to pass the verification. Then, the scenarios after the preventive control are further deduced and updated.

Step 2: based on the latest scenario, the result of the restoration operation is sampled. If the operation fails, then generate the emergency or correction control measures and costs [34], deduce and update the scenario, and adaptively switch to an alternative path to simulate the subsequent restoration control of the restoration target. On the contrary, if the operation is successful, the subsequent scenario is directly deduced and updated.

Step 3: *Step 1* and *Step 2* are repeated until the simulation of the restoration process of the path is completed. Afterwards, the overall restoration income I_i^k, restoration cost C_i^k, and security control cost E_i^k of the deterministic process i are evaluated. I_i^k includes the unit restoration income and load restoration income which are evaluated using (16) and (2), respectively; C_i^k is evaluated using (3); and E_i^k is the total cost of emergency and correction control in this process.

Step 4: *Step 1*-*Step 3* are repeated to generate several deterministic restoration processes. Then, the expected restoration income I^k, expected restoration cost C^k, and path security risk R^k in Section II-B are evaluated by using (18)-(20), respectively, and the restoration path is optimized according to the expected net income I^k-C^k-R^k.

$$I^k = \sum_{i=1}^{N_P} \frac{I_i^k}{N_P} \tag{18}$$

$$C^k = \sum_{i=1}^{N_P} \frac{C_i^k}{N_P} \tag{19}$$

$$R^k = \sum_{i=1}^{N_P} \frac{E_i^k}{N_P} \tag{20}$$

where N_P is the total number of the simulated deterministic restoration processes.

IV. Simulation Results and Analysis

In order to verify the effectiveness of the proposed framework and method in this paper, a prototype DRDSS using C++ is developed. The simulation test system is built with its topological connection referring to that of IEEE 123-node system [35]. There are 123 nodes in this test system, among which the nodes 1-3 serve as TDBs, the nodes 35, 39, 43, 65, 90, 105, and 111 serve as T-type nodes, and other nodes are connected with loads or DGs. It has been assumed that T-type nodes cannot be isolated alone because there is no switch on both sides of it, while all the other nodes can be isolated alone by the switches beside it. There are four units in the system, i.e., G1, G2, G3, and G4, connected to nodes 4, 52, 79, and 110, respectively. The system topology, load data of each node before power outage, technical parameters of the units in distribution system, and simulation parameters are presented in Appendix A. All simulations are performed on a personal computer with Intel Core i5-3470 CPU @3.20 GHz and 8 GB RAM. The computation time is dependent on the setting of calculation conditions and the outage scenarios.

It is assumed that the power system starts the restoration process at 00:00 after a large-scale power outage. At this time, the available power supply sources of the distribution system are: ① the power delivery from the transmission system at node 1, and its power delivery plan curve P_1 is presented in Fig. 6(a); ② black-start unit G3 of the distribution system, which restarts successfully and provides 15 MW; and ③ black-start unit G4 of the distribution system, which restarts successfully and provides 10 MW.

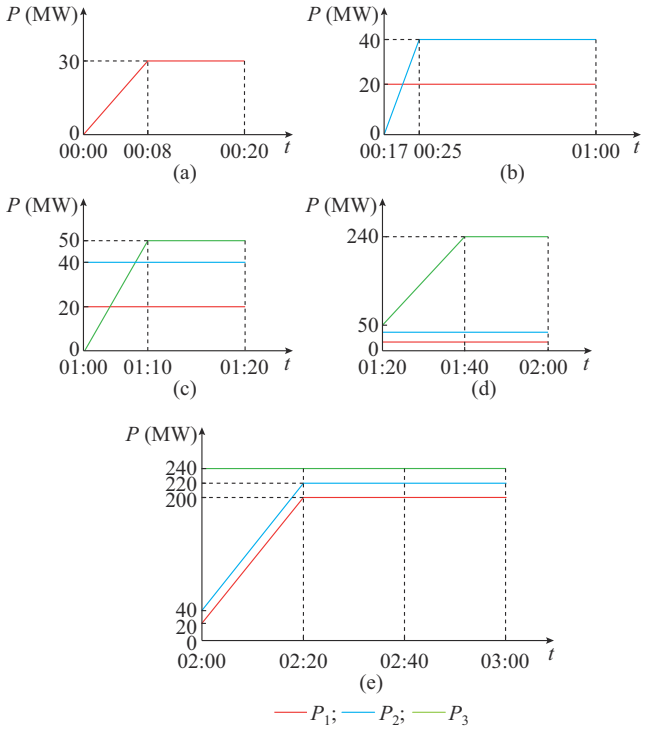

Fig. 6. Power delivery plan curves of transmission system. (a) Update at 00:00. (b) Update at 00:17. (c) Update at 01:00. (d) Update at 01:20. (e) Update at 02:00.

A. Adaptive Optimization and Execution of Distribution System Restoration Scheme

Based on the initial power outage scenario at 00:00, the adaptive management and control module of the restoration process in the proposed DRDSS initiates the first-time optimization of the restoration schemes and sends the first-time optimization instruction to the dynamic partitioning module in the upper layer. The restoration schemes are optimized as follows.

1) In the upper layer, the optimization submodule of pre-adjustment scheme of operation mode is unable to find a feasible transfer scheme for the energized loads. Further, based on the real-time power outage scenario, the partition adjustment submodule determines partitions 1-3 with node 1, G3, and G4 as the roots of the energized power grids, respectively. Finally, the decision-making submodule of inter-partition

connectivity recommends no BNPs for inter-partition connectivity and sends the partitioning result to the lower-partition optimization layer.

2) In the lower layer, the table of alternative restoration scheme of each partition is optimized in parallel by the optimization module of restoration scheme of each partition. Then, these tables are sent to the decision-making submodule of inter-partition connectivity in the upper layer.

3) In the upper layer, the decision-making submodule of inter-partition connectivity optimizes the inter-partition connectivity schemes after obtaining the alternative restoration plan tables of the three partitions. Since there is no suggestion on inter-partition connectivity, the scheme with the largest expected net income per unit of power consumption in the table of alternative restoration scheme table of each partition is chosen as the optimal one of each partition.

The optimal restoration schemes of the first few steps of each partition are presented in Table I, and the restoration operations of each partition are executed separately and parallelly. The adaptive management and control module of the restoration process of the proposed DRDSS continues to monitor the outage scenario of the distribution system and the restoration process of these three partitions. The lower partition-optimization layer continues to dynamically expand the subsequent restoration schemes of each partition.

TABLE I
OPTIMAL RESTORATION SCHEMES OF THREE PARTITIONS (OPTIMIZATION RESULTS AT 00:00)

No.	Estimated completed time	Partition No.	Restoration path	Restoration power (MW)	Restoration target	
					Unit	Load node
1	00:06	2	G3-79-87	5		87
2	00:07	3	G4-110-101	5		101
3	00:08	1	1-7-16-27-36-45-52-G2	2	G2	
4	00:12	2	87-97-107	5		107
5	00:12	3	110-120	4		120
6	00:14	1	36-35-34-33-42-41	5		41
7	00:17	1	33-32-20	5		20
⋮	⋮	⋮	⋮	⋮	⋮	⋮

The power outage scenario before re-optimization at 00:17 is presented in Fig. 7, where S_i is the restoration scheme of step i. At this time, the restoration schemes of partitions 2 and 3 have been executed, forming two stable energized power grids. In the restoration process, partition 1 encounters a permanent line fault in the process of restoring line 33-42. An alternative restoration path, i. e., 35-44-43-42-41, is chosen to continue the restoration of target node 41. However, the completion time of its load restoration is delayed from 00:14 to 00:17. The estimated completion time of the subsequent schemes within this partition is also delayed accordingly, whereas the restoration processes of partitions 2 and 3 are not affected.

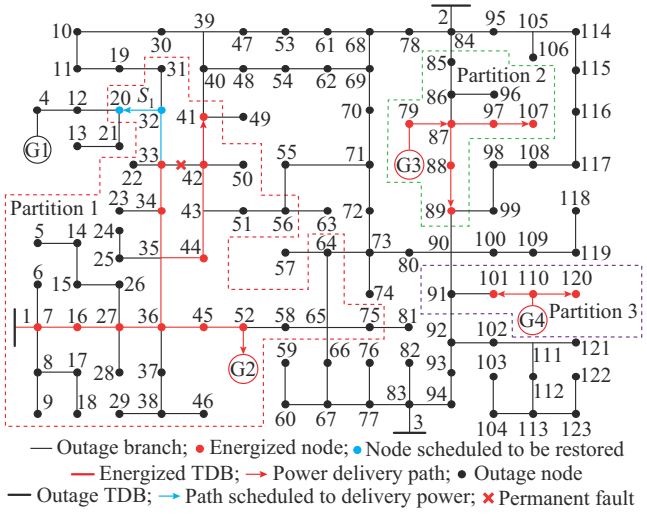

Fig. 7. Power outage scenario before re-optimization at 00:17.

At 00:17, the power delivery plan curves from the transmission system to the distribution system at TDBs are updated on the transmission system side, as shown in Fig. 6(b). The upper limit of power delivery plan at node 1 is reduced from the original 30 MW to 20 MW, and a new power delivery plan curve P_2 with the upper limit of 40 MW is added at node 2. The adaptive management and control module of the restoration process in the proposed DRDSS fails to find a feasible alternative scheme for this. Therefore, it suspends the operations of the subsequent restoration schemes of partition 1 and triggers the re-optimization of restoration schemes of all partitions.

The multi-partition restoration schemes after re-optimization are presented in Fig. 8. When the partition adjustment submodule determines the partition of each energized power grid, there are overlapping areas among the partitions of energized power grids with node 1, node 2, and G3 as their roots. Therefore, based on the branch restoration value, the nodes such as 10, 40, 51, 55, 63, and 86 in the overlapping area are assigned to partition 4 formed by node 2. The next restoration targets of partitions 1 and 4 are nodes 20 and 86, respectively. Partitions 2 and 3 have no other restoration targets as they are constrained by the spinning reserve capacity.

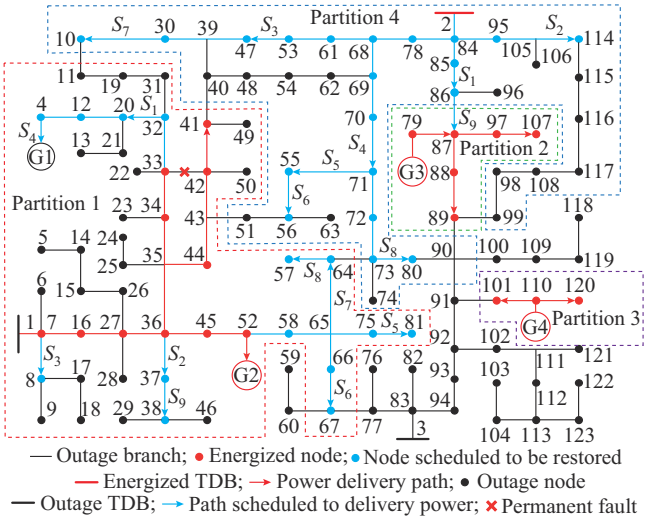

Fig. 8. Multi-partition restoration schemes after re-optimization at 00:17.

At 00:49, partitions 2 and 4 satisfy the inter-partition connectivity conditions and perform the connectivity operation. The partitioning result obtained after re-optimization at 00:49 is presented in Fig. 9. Due to the constraint of spinning reserve capacity, there is no subsequent restoration scheme for each partition.

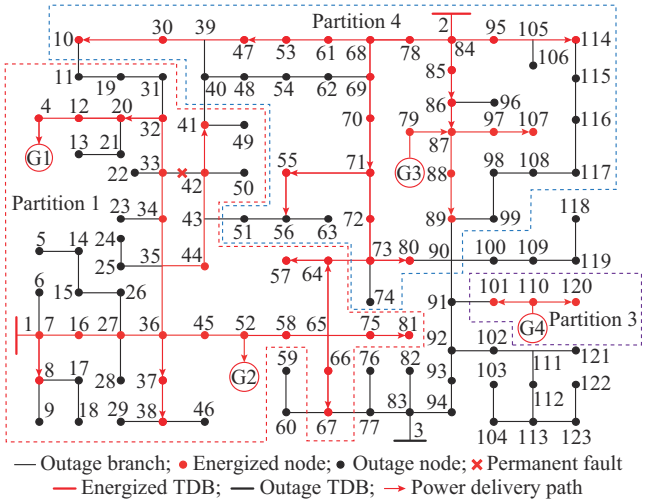

Fig. 9. Partitioning result after re-optimization at 00:49.

At 01:00, the power delivery plan curves from the transmission system to the distribution system at TDBs are updated, as shown in Fig. 6(c). A power delivery plan curve P_3 with the upper limit of 50 MW is newly added at node 3, whereas the power delivery plan curves at nodes 1 and 2 remain unchanged. The adaptive management and control module of the restoration process in the proposed DRDSS triggers the re-optimization of restoration schemes of all the partitions and obtains the restoration scheme of each partition, as shown in Fig. 10.

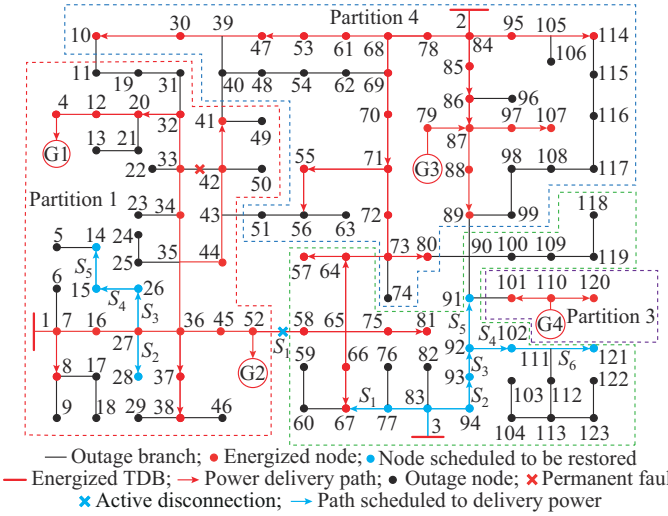

Fig. 10. Multi-partition restoration scheme after re-optimization at 01:00.

Based on the current outage scenario, the optimization submodule of pre-adjustment scheme of operation mode generates several alternative energized load transfer schemes, and deduces the corresponding hypothetical scenarios after the load transfer. The partition adjustment submodule selects closing path 3-83-77-67 and opening path 52-58 as the optimal energized load transfer scheme, which transfers the power-supplied subtree originally in partition 1 to node 3, and readjusts the partitions. Based on this, partition 1 frees up the power of about 20 MW to restore important targets such as the load at node 28. The next restoration target of partition 5 is node 93. Please note that partitions 3 and 4 have no subsequent restoration scheme due to the constraint of spinning reserve capacity.

The proposed DRDSS continuously coordinates the implementation process and optimization process of the restoration schemes according to the updated power delivery plan curves generated at transmission system side shown in Fig. 6(d) and (e) until the restoration of distribution system is completed. The completion of the whole process takes 2 hours and 49 min. The information of the complete restoration process and the topology of the restored system are presented in Appendix B. The decision-making and execution process of the aforementioned restoration schemes shows that the proposed DRDSS can adapt to the space-time distribution characteristics of power delivery plan between transmission and distribution systems, load capacity, and restoration income per unit load. In addition, the proposed DRDSS can generate a set of hypothetical scenarios through optimizing the pre-adjustment scheme of operation mode based on real-time outage scenario. It can also dynamically coordinate the restoration decision-making space of multiple types of power supplies such as the power delivery from transmission system at TDBs and the black-start units in the distribution system, through increasing the number of partitions, adjusting the partitions, and connecting partitions to enhance the concurrent restoration income of each partition.

B. Comparison with Method 1 Without Pre-adjustment of Operation Mode

The proposed method for pre-adjustment optimization of operation mode in the dynamic partitioning module of the upper layer of DRDSS is compared with the comparison method 1. The comparison method 1 is set based on the decision-making framework presented in this paper, whereas the restoration scheme optimization is performed only based on the real-time outage scenario [21], without pre-adjustment of operation mode.

The net income curves of the restoration schemes obtained by the proposed DRDSS and the comparison method 1 are presented in Fig. 11. It is notable that by 02:49, the actual net income of the proposed pre-adjustment optimization method of operation mode increases by 8.3% compared with the comparison method 1.

The node 1 and node 2 obtain the power supply from the transmission system early at 00:00 and 00:17, respectively. At 00:49, two large power-supplied trees are formed in partitions 1 and 4, as presented in Fig. 9, in which some important loads located in the vicinity of node 3 have been restored. As there is no more available power, it is impossible to further restore the remaining-to-be-restored loads in each

partition. At 01:00, the node 3 receives a large power support from the transmission system. However, the remaining-to-be-restored loads in its recoverable outage area are small and not very important, and it is unable to connect with the power-supplied tree in partition 1 or 4 due to the open-loop operation constraint. Therefore, the restoration income that can be generated by the available power is severely limited. If the comparison method 1 without pre-adjustment of operation mode is adopted, the power delivery from transmission system at node 3 can only be used to restore the loads in a very small partition area of node 3. At the same time, more important remaining-to-be-restored loads in partition 1 or 4 cannot be restored in time. This reduces the overall load restoration income of the distribution system. On the contrary, if the proposed pre-adjustment scheme optimization method of operation mode is adopted, it transfers the power-supplied subtree with node 58 as its root, which originally belongs to partition 1, to node 3 by closing path 3-83-77-67 and opening branch 52-58. Consequently, partition 1 frees up 20 MW available power to restore the important loads carried by nodes 28 and 26, while node 3 still has available power to restore the remaining-to-be-restored loads in its partition.

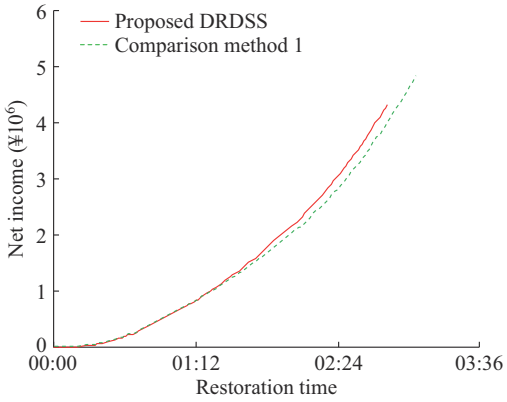

Fig. 11. Net incomes of proposed DRDSS and comparison method 1.

The time that the transmission system delivers power to different TDBs is usually quite different. This makes the scale and restoration ability of each energized power grid different during the restoration process of the distribution system. This is not conducive to the improvement of the overall restoration income. The aforementioned examples show that by using the flexibility of network topology adjustment of the closed-loop designed distribution system, the pre-adjustment of operation mode by using energized load transfer can coordinate the restoration decision-making space of each partition, reduce the outage duration of important targets, and improve the global restoration income.

C. Comparison with Method 2 Without Dynamic Partitioning

The dynamic partitioning method in the upper layer of the proposed DRDSS is compared with the comparison method 2. The comparison method 2 is set based on the decision-making framework presented in this paper. However, the partitions are determined by the power-supplied tree of each TDB during normal operation [14], without pre-adjustment and partition adjustment of operation mode.

The net income curves of restoration schemes obtained by the proposed DRDSS and the comparison method 2 are presented in Fig. 12. It is notable that by 02:49, the actual net income of the proposed dynamic partitioning method presented in this paper increases by 8.3% compared with the comparison method 2.

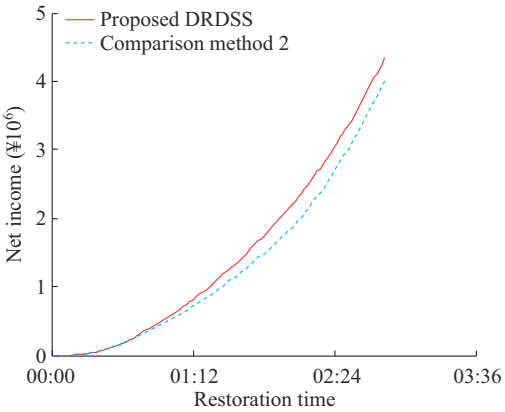

Fig. 12. Net incomes of restoration schemes obtained by proposed DRDSS and comparison method 2.

Based on the power-supplied tree of each TDB during the normal operation as presented in Fig. A1 of Appendix A, the partitions are determined according to comparison method 2, which makes it impossible to restore important loads at node 41 until node 2 gets power supply from the transmission system at 00:17. Similarly, it is not possible to restore the important loads at nodes 67 and 81 until node 3 receives power supply from the transmission system at 01:00. However, when the proposed dynamic partitioning method is adopted, after node 1 receives power supply from the transmission system, nodes 41, 67, and 81 are included in the partition of node 1, so important loads at these nodes can be restored in advance, thus reducing the power outage losses. Similarly, when nodes 2 and 3 get power supplies from the transmission system successively, the scope of each partition will be dynamically adjusted, and the power supply utilization will be coordinated through the pre-adjustment scheme optimization of operation mode.

The aforementioned results show that as compared with the comparison method 2, the proposed dynamic partitioning method dynamically adjusts the number of partitions and the scope of each partition according to the actual available power of each energized power grid and the restoration requirement of each node, thus ensuring the timely restoration of important targets and improving the overall restoration income.

D. Comparison with Method 3 Without Security Risk

The proposed security risk based restoration scheme optimization for each partition in the lower layer of the proposed DRDSS is compared with the comparison method 3. The comparison method 3 is set based on the decision-making framework presented in this paper, but without security

risk of restoration path in the intra-partition restoration scheme optimization [8].

The net income curves of restoration schemes obtained by the proposed DRDSS and the comparison method 3 are presented in Fig. 13, which is calculated based on the numerical simulation process of restoration execution. All uncertain events with security risks will be determined with the implementation of execution simulation process, and the security risk in the calculation of net income decision-making model of the restoration control will be reflected as the determined cost. It is notable that by 02:49, the actual net income of the proposed security risk based restoration scheme optimization method increases by 4.7% compared with the comparison method 3.

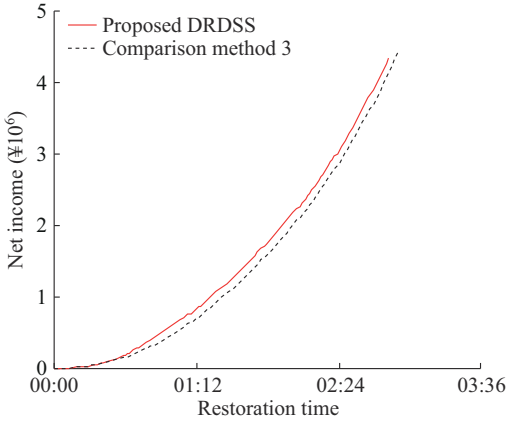

Fig. 13. Net incomes of restoration schemes obtained by proposed DRDSS and comparison method 3.

Although there are important remaining-to-be-restored loads at nodes 14, 15, 25, and 26, the high fault probabilities of the branches 15-26, 26-27, and 25-35 in the early stage of restoration make the restoration schemes of delivering power to those nodes have high security risks and low net restoration incomes. Therefore, in this paper, the restoration of nodes 14, 15, 25, and 26 is not given priority. Instead, the targets such as nodes 20 and 41 are chosen for restoration. Until the power delivery security risks of nodes 14 and 15 are reduced in the later stage of the process, the restoration schemes of these targets are suggested. When the comparison method 3 is adopted, the nodes 14, 15, 25, and 26 in partition 1 are restored first. However, in the actual restoration process of the power delivery path, several branches fail to close one after another, resulting in the repeated power outages of multiple lines. In this paper, it is set that each of the failed branches needs to close several times and finally succeed, resulting in about 10-min delay for each branch. This significantly delays the restoration time of the subsequent nodes, thus reducing the overall restoration income of the distribution system.

The aforementioned results show that, in terms of the evaluation of restoration path, actively taking the influence of the uncertainty of restoration process into account through security risk assessment enables us to effectively avoid the uncertain security problems caused by the restoration operations, thus improving the actual restoration income.

V. Conclusion

Based on the previous research regarding the transmission system restoration control of our research group, this paper establishes the risk optimization model for restoration control of distribution system and proposes a two-layer decision-making framework for adaptive restoration control of distribution system. The upper layer of the proposed framework firstly optimizes the pre-adjustment schemes of operation mode timely to generate a set of hypothetical scenarios, which can produce greater expected restoration income for the subsequent partitioning optimization in the restoration process. Then, the restoration partition of each energized power grid is adjusted with the guidance of the branch restoration value, and the space-time decision-making of inter-partition connectivity is made, thus the restoration decision-making space of each energized power grid can be planned from a global perspective. The lower layer of the proposed system optimizes the restoration schemes of units and loads in each partition concurrently, where the costs of security control and security risk are considered during the evaluation of the restoration scheme, instead of only considering the income of the restoration scheme. Consequently, the restoration scheme can be evaluated more comprehensively. In the actual restoration process, the restoration schemes are adaptively adjusted against any uncertain event and its security control measures. The decision support system also provides the information interaction interface necessary for collaborative restoration with the related transmission system. The simulation results show the effectiveness and adaptability of the proposed framework against various uncertainties such as power failure scenario uncertainties.

Appendix A

The topology of the 123-node test system, load data of each node before power outage, technical parameters of units in the system, and simulation parameters are presented in this section.

The topology of the 123-node test system and its operation mode before power outage are presented in Fig. A1. Without loss of generality, the load at each node is set to be 5 MW, and the total active power of load before outage is set to be 565 MW. All the loads are controllable. The restoration income per unit load ranges between [0, 1.0], and the unit is 10000 ¥/MWh. It is assumed that all the equipment can be restored after the power outage. The restoration time required for each branch is 1 min. Before 01:00, the probability of various faults for lines 14-15, 25-35, and 26-27 is 0.75. The probability of various faults for other equipment is 0.002. After 01:00, the probability of various faults for all the equipment is 0.0001. β_{GP}, β_{GN}, and β_{BL} are all set to be 0.95. Let $\gamma = 0.1$ and $\zeta = 0.1$. The preset end time of evaluation is 10:00. The upper and lower limits of node voltage are 1.1 p.u. and 0.9 p.u., respectively.

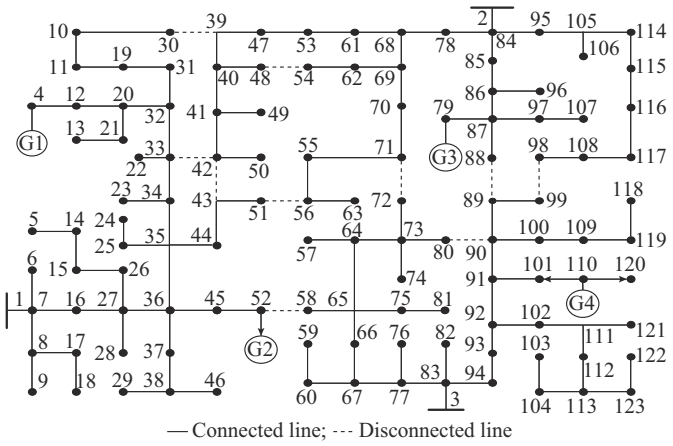

Fig. A1. Topology of 123-node test system.

The technical parameters of units G1, G2, G3, and G4 are presented in Table AI, where P_G^N, P_G^{st}, P_G^{th}, Q_G^{max}, Q_G^{min}, and T_G^{cold} denote rated active power capacity, start-up power demand, the minimum technical output, the upper limit of reactive power, the lower limit of reactive power, and the minimum cold restarting time of a unit, respectively; R_G is the ramping rate; Y or N represents that the unit is or is not a black-start unit, respectively; and T and H represent that the thermal power unit and hydropower unit, respectively.

TABLE AI
TECHNICAL PARAMETERS OF DISTRIBUTION SYSTEM UNITS

Unit	P_G^N (MW)	P_G^{st} (MW)	P_G^{th} (MW)	Q_G^{max} (Mvar)	Q_G^{min} (Mvar)	T_G^{cold} (min)	R_G (MW /min)	Black start	Type
G1	10.0	1.0	5.0	7.5	−4.5	5	1.0	N	T
G2	20.0	2.0	10.0	14.0	−10.0	5	1.5	N	T
G3	15.0	0.0	0.0	10.0	−7.0	0	3.5	Y	H
G4	10.0	0.0	0.0	7.5	−4.5	0	3.5	Y	H

APPENDIX B

In this section, the entire restoration process of the case studied in this paper is presented. The topological structure diagram after restoration is presented in Fig. B1. The restoration details are presented in Table BI.

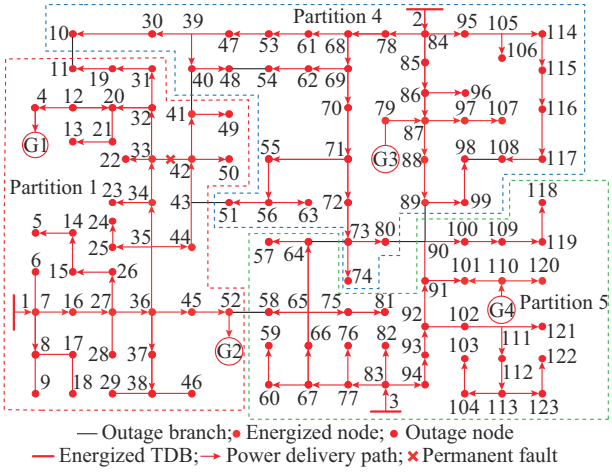

Fig. B1. Topological structure diagram after restoration.

TABLE BI
ENTIRE RESTORATION PROCESS OF STUDIED CASE

No.	Estimated completed time	Partition No.	Restoration path	Restoration power (MW)	Restoration target	
					Unit	Load node
1	00:06	2	G3-79-87	5.0		87
2	00:07	3	G4-110-101	5.0		101
3	00:08	1	1-7-16-27-36-45-52-G2	2.0	G2	
4	00:12	2	87-97-107	5.0		107
5	00:12	3	110-120	4.0		120
6	00:17	1	36-35-34-33-44-43-42-41	5.0		41
7	00:17	2	87-88-89	3.5		89
8	00:20	1	33-32-20	5.0		20
9	00:21	4	2-84-85-86	5.0		86
10	00:22	1	36-37	5.0		37
11	00:24	1	7-8	5.0		8
12	00:25	4	84-95-105-114	5.0		114
13	00:28	1	20-12-4-G1	1.0	G1	
14	00:31	4	84-78-68-61-53-47	5.0		47
15	00:33	1	52-58-65-75-81	5.0		81
16	00:35	4	68-69-70-71	5.0		71
17	00:36	1	65-66-67	5.0		67
18	00:37	4	71-55	5.0		55
19	00:38	1	65-64	5.0		64
20	00:39	4	55-56	5.0		56
21	00:40	1	64-57	5.0		57
22	00:42	1	37-38	5.0		38
23	00:43	4	47-39-30-10	5.0		10
24	00:47	4	71-72-73-80	5.0		80
25	00:49	2, 4	86-87 (inter-partition connectivity)			
26	01:04	1, 4	3-83-77-67			
27	01:06	1, 4	Open 52-58 (energized load transfer)			
28	01:08	1	27-28	5.0		28
29	01:09	5	3-94-93	5.0		93
30	01:10	1	27-26	5.0		26
31	01:11	5	93-92	5.0		92
32	01:12	1	26-15	5.0		15
33	01:13	5	92-102	5.0		102
34	01:14	1	15-14	5.0		14
35	01:15	5	92-91	5.0		91
36	01:18	5	102-111-121	5.0		121
⋮	⋮	⋮	⋮	⋮	⋮	⋮
122	02:49	1	52	5.0		52

REFERENCES

[1] Y. Xue, H. Wang, Z. Dong *et al.*, "A review on restorative control in interconnected grids under electricity market environment," *Automation of Electric Power Systems*, vol. 31, no. 21, pp. 110-115, Nov. 2007.

[2] F. Shen, Q. Wu, and Y. Xue, "Review of service restoration for distri-

bution networks," *Journal of Modern Power Systems and Clean Energy*, vol. 8, no. 1, pp. 1-14, Jan. 2020.
[3] R. R. Nejad and W. Sun, "Distributed load restoration in unbalanced active distribution systems," *IEEE Transactions on Smart Grid*, vol. 10, no. 5, pp. 5759-5769, Sept. 2019.
[4] B. Chen, C. Chen, J. Wang *et al*., "Sequential service restoration for unbalanced distribution systems and microgrids," *IEEE Transactions on Power Systems*, vol. 33, no. 2, pp. 1507-1520, Mar. 2018.
[5] Y. Xu, C. Liu, K. P. Schneider *et al*., "Microgrids for service restoration to critical load in a resilient distribution system," *IEEE Transactions on Smart Grid*, vol. 9, no. 1, pp. 426-437, Jan. 2018.
[6] *IEEE Standard for Distributed Resources Interconnected with Electric Power Systems*, IEEE Standard 1547.2-2008.
[7] W. Li, Y. Li, C. Chen *et al*., "A full decentralized multi-agent service restoration for distribution network with DGs," *IEEE Transactions on Smart Grid*, vol. 11, no. 2, pp. 1100-1111, Mar. 2020.
[8] J. Li, X. Ma, C. Liu *et al*., "Distribution system restoration with microgrids using spanning tree search," *IEEE Transactions on Power Systems*, vol. 29, no. 6, pp. 3021-3029, Nov. 2014.
[9] R. E. Perez-Guerrero and G. T. Heydt, "Distribution system restoration via subgradient-based Lagrangian relaxation," *IEEE Transactions on Power Systems*, vol. 23, no. 3, pp. 1162-1169, Aug. 2008.
[10] A. Sharma, D. Srinivasan, and A. Trivedi, "A decentralized multiagent system approach for service restoration using DG islanding," *IEEE Transactions on Smart Grid*, vol. 6, no. 6, pp. 2784-2793, Nov. 2015.
[11] P. L. Cavalcante, J. C. Lopez, J. F. Franco *et al*., "Centralized self-healing scheme for electrical distribution systems," *IEEE Transactions on Smart Grid*, vol. 7, no. 1, pp. 145-155, Jan. 2016.
[12] C. Liu, S. J. Lee, and S. S. Venkata, "An expert system operational aid for restoration and loss reduction of distribution systems," *IEEE Transactions on Power Systems*, vol. 3, no. 2, pp. 619-626, May 1988.
[13] S. Toune, H. Fudo, T. Genji *et al*., "Comparative study of modern heuristic algorithms to service restoration in distribution systems," *IEEE Transactions on Power Delivery*, vol. 17, no. 1, pp. 173-181, Jan. 2002.
[14] R. R. Nejad, W. Sun, and A. Golshani, "Distributed restoration for integrated transmission and distribution system with DERs," *IEEE Transactions on Power Systems*, vol. 34, no. 6, pp. 4964-4973, Nov. 2019.
[15] J. Zhu and Y. Xue, "An expert system for restoration of distribution system," *Automation of Electric Power Systems*, vol. 15, no. 3, pp. 22-28, Apr. 1991.
[16] F. Wang, C. Chen, C. Li *et al*., "A multi-stage restoration method for medium-voltage distribution system with DGs," *IEEE Transactions on Smart Grid*, vol. 8, no. 6, pp. 2627-2636, Nov. 2017.
[17] X. Huang, Y. Yang, and G. A. Taylor, "Service restoration of distribution systems under distributed generation scenarios," *CSEE Journal of Power and Energy Systems*, vol. 2, no. 3, pp. 43-50, Sept. 2016.
[18] Z. Bie, Y. Lin, G. Li *et al*., "Battling the extreme: a study on the power system resilience," *Proceedings of the IEEE*, vol. 105, no. 7, pp. 1253-1266, Jul. 2017.
[19] T. Zhou, L. Hao, H. Wang *et al*., "Unscheduled outage restoration strategy of Active distribution network considering risk and gain," *Automation of Electric Power Systems*, vol. 42, no. 13, pp. 136-144, Jul. 2018.
[20] B. Chen, C. Chen, J. Wang *et al*., "Multi-time step service restoration for advanced distribution systems and microgrids," *IEEE Transactions on Smart Grid*, vol. 9, no. 6, pp. 6793-6805, Nov. 2018.
[21] Z. Li, Y. Xue, H. Wang *et al*., "Decision support system for adaptive restoration control of transmission system," *Journal of Modern Power Systems and Clean Energy*, vol. 9, no. 4, pp. 870-885, Jul. 2021.
[22] Q. Zhang, J. Zhao, Z. Dai *et al*., "Distributed coordinated optimization method for black-start of transmission and distribution networks based on analytical target cascading," *Automation of Electric Power Systems*, vol. 45, no. 3, pp. 111-120, Feb. 2021.
[23] L. Hao, C. Chen, C. Wang *et al*., "Restoration control strategy of distribution network based on dynamic evaluation of restoration value," *Electric Power Automation Equipment*, vol. 41, no. 7, pp. 73-80, Jul. 2021.
[24] P. Wang and R. Billinton, "Time sequential distribution system reliability worth analysis considering time varying load and cost models," *IEEE Transactions on Power Delivery*, vol 14, no. 3, pp. 1046-1051, Jul. 1999.
[25] F. Bu, K. Dehghanpour, Z. Wang *et al*., "A data-driven framework for assessing cold load pick-up demand in service restoration," *IEEE Transactions on Power Systems*, vol. 34, no. 6, pp. 4739-4750, Nov. 2019.
[26] K. P. Schneider, J. C. Fuller, and D. P. Chassin, "Multi-state load models for distribution system analysis," *IEEE Transactions on Power System*, vol. 26, no. 4, pp. 2425–2433, Nov. 2011.
[27] K. McKenna and A. Keane, "Residential load modeling of price-based demand response for network impact studies," *IEEE Transactions on Smart Grid*, vol. 7, no. 5, pp. 2285-2294, Sept. 2016.
[28] S. Khushalani, J. M. Solanki, and N. N. Schulz, "Optimized restoration of unbalanced distribution systems," *IEEE Transactions on Power Systems*, vol. 22, no. 2, pp. 624-630, May 2007.
[29] Y. Xue, "Space-time cooperative framework for defending blackouts: part I from isolated defense lines to coordinated defending," *Automation of Electric Power Systems*, vol. 30, no. 1, pp. 8-16, Jan. 2006.
[30] L. Ding, Z. Pan, and W. Cong, "Searching for intentional islanding strategies of distributed generation based on rooted tree," *Proceedings of the CSEE*, vol. 28, no. 25, pp. 62-67, Sept. 2008.
[31] J. Liu, Q. Sun, X. Zhang *et al*., "Analysis on and criteria for loop closing operation for distribution grids," *Automation of Electric Power Systems*, vol. 38, no. 11, pp. 130-135, Jun. 2014.
[32] Z. Liu, W. Xia, and M. Liu, "Distributed generator self-organized network strategy applied to microgrid service restoration," *Automation of Electric Power Systems*, vol. 39, no. 9, pp. 192-199, May 2015.
[33] Y. Xue and Z. Wang, "Optimization of preventive control for transient voltage security," *Automation of Electric Power Systems*, vol. 30, no. 9, pp. 1-4, May 2006.
[34] Y. Xue, D. Wang, Q. Wu *et al*., "A review on optimization and coordination of emergency control and correction control," *Automation of Electric Power Systems*, vol. 33, no. 12, pp. 1-7, Jun. 2009.
[35] S. Lei, J. Wang, and Y. Hou, "Remote-controlled switch allocation enabling prompt restoration of distribution systems," *IEEE Transactions on Power Systems*, vol. 33, no. 3, pp. 3129-3142, May 2018.

Lili Hao received the B.E. and M.E. degrees from Hohai University, Nanjing, China, in 2001 and 2004, respectively, and the Ph. D. degree from Southeast University, Nanjing, China, in 2010, all in electrical engineering. She was a Visiting Scholar in the School of Electrical Engineering and Computer Science, Washington State University, Pullman, USA, from 2015 to 2016. She is currently an Assistant Professor at Nanjing Tech University, Nanjing, China. Her research interests include power system security and reliability.

Yusheng Xue received the B.E. degree from Shandong University, Jinan, China, in 1963, the M.E. degree from State Grid Electric Power Research Institute, Nanjing, China, in 1981, and the Ph.D. degree in electrical engineering from University of Liège, Liège, Belgium, in 1987. He is the Member of Chinese Academy of Engineering. He is the Honorary President of State Grid Electric Power Research Institute (NARI Group Corporation), Nanjing, China. His research interests include power system stability control, security, and economic operation.

Ze Li received the B.E. and Ph.D. degrees from Southeast University, Nanjing, China, in 2014 and 2021, respectively, all in electrical engineering. He is an Engineer of State Grid Electric Power Research Institute (NARI Group Corporation), Nanjing, China. His research interests include power system security and reliability.

Haohao Wang received the B.E. degree from Hohai University, Nanjing, China, in 2001, and the Ph.D. degree from Southeast University, Nanjing, China, in 2007, all in electrical engineering. He is currently a Professorate Senior Engineer of State Grid Electric Power Research Institute (NARI Group Corporation), Nanjing, China. His research interests include power system security and reliability.

Qun Xu received the B.E. and M.E. degrees from Shandong University of Technology, Jinan, China, in 1989 and 1992, respectively, and the Ph.D. degree from Shandong University, Jinan, China, in 2004, all in electrical engineering. He is currently a Professorate Senior Engineer of State Grid Qingdao Power Supply Company, Qingdao, China. His research interests include power system dispatching automation.